ICARUS 12, 10–45 (1970)

Television Experiment for Mariner Mars 1971[1]

H. MASURSKY, R. BATSON, W. BORGESON, M. CARR, J. McCAULEY, D. MILTON, R. WILDEY, AND D. WILHELMS
U.S. Geological Survey, Flagstaff, Arizona, and Menlo Park, California

B. MURRAY, N. HOROWITZ, R. LEIGHTON, AND R. SHARP
California Institute of Technology, Pasadena, California

W. THOMPSON, G. BRIGGS, P. CHANDEYSSON, AND E. SHIPLEY
Bellcomm, Inc., Washington, D.C.

C. SAGAN AND J. POLLACK
Cornell University, Ithaca, New York

J. LEDERBERG AND E. LEVINTHAL
Stanford University, Stanford, California

W. HARTMANN
University of Arizona, Tucson, Arizona

T. McCORD
Massachusetts Institute of Technology, Cambridge, Massachusetts

B. SMITH
New Mexico State University, Las Cruces, New Mexico

M. DAVIES
Rand Corporation, Santa Monica, California

G. DE VAUCOULEURS
University of Texas, Austin, Texas

C. LEOVY
University of Washington, Seattle, Washington

Received December 11, 1969; Revised January 14, 1970

The Television Experiment objectives are to provide imaging data which will complement previously gathered data and extend our knowledge of Mars. The two types of investigations will be fixed-feature (for mapping) and variable-feature (for surface and atmospheric changes). Two cameras with a factor-of-ten difference in resolution will be used on each spacecraft for medium- and high-resolution imagery. Mapping of 70% of the planet's surface will be provided by medium-resolution imagery. Spot coverage of about 5% of the surface will be possible with the high-resolution imagery.

The experiment's 5 Principal Investigators and 21 Co-Investigators are organized into a team. Scientific disciplines and technical task groups have been formed to provide the formulation of experiment requirements for mission planning and instrument development. It is expected that the team concept will continue through the operational and reporting phases of the Mariner Mars 1971 Project.

[1] This work was performed for the Jet Propulsion Laboratory, California Institute of Technology, sponsored by the National Aeronautics and Space Administration, under Contract No. NAS 7-100.

I. Introduction

The primary objective of the television experiment on Mariner Mars 1971 is to provide imaging data that will increase scientific knowledge of Mars and the solar system. This objective can be defined further:

(1) To investigate various Martian phenomena in order to achieve a more complete understanding of the dynamics, history, environment, and surface physiography of the planet.

(2) To obtain imagery suitable for development of better geologic, dynamic, and topographic maps of the planet in anticipation of choosing areas for more intensive investigations, which will, in later planetary programs, culminate in landings on the surface.

Although the experiment is not expected to provide direct information regarding the possibility of life, it is expected that it will provide indirect evidence on the suitability of Mars as a habitat for life.

1. *Preinsertion Sequence*

Mariners VI and VII (Mariner Mars 1969) took 50 and 93 pictures, respectively, of the full planetary disk during approach starting at distances of about 1.2 and 1.8 million km, respectively. A similar preinsertion sequence is planned for the two spacecraft of Mariner Mars 1971. Not only will this allow geologic and topographic surveillance of the whole planet, but, more important, will provide new information on the changed appearance of Mars in 1971, allowing better planning of the orbital picture-taking sequences. The Martian season during the mission will be different from that during the 1969 encounters; it will be more like that observed telescopically in 1958. The preinsertion sequence will provide higher-resolution images than do the Earth-based photographs, and will help to optimize the orbital photographic sequences. When compared with Mariner VI and VII pre-encounter pictures, this preinsertion sequence also will provide early *scientific* data pertaining to changes of Martian features.

2. *Orbital Scientific Objectives*

The television studies in orbit consist of two types of scientific investigations: fixed-features and variable-features. In the fixed-features investigation, the surface features will be seen at greater resolution than possible from observations by telescope from Earth and more completely than by Mariners IV, VI, and VII.

The objectives of the fixed-features investigation are as follows:

(1) To obtain a broad range of image information to be used for regional stratigraphic studies of tectonic features, crater configuration and distribution, and local surface environments.

(2) To measure, by photometric and photogrammetric analysis, surface slopes and elevations; to determine surface brightness and albedo differences; and to perform analyses related to improving the accuracy of the photometric function for various regions on Mars.

(3) To obtain improved values for the figure of the planet and thereby investigate possible departures from hydrostatic equilibrium.

(4) To study the surface characteristics of Phobos and Deimos.

The variable-features investigation will study time-variable phenomena on the surface and in the atmosphere of Mars in order to obtain information on atmospheric structure and circulation, details of diurnal and seasonal changes, and clues regarding the possibility of life on Mars. The specific phenomena to be studied are the following:

(1) The "wave of darkening."

(2) Polar caps and cap-edge phenomena.

(3) Nightside atmospheric and surface fluorescence.

(4) Haze in the atmosphere.

(5) White "clouds" in nonpolar regions.

(6) Dust clouds and dust storms.

(7) Phenomena of possible exobiological significance.

Details of these investigations and a description of the Mariner Mars 1971 television subsystem are presented in the following sections of this paper.

TABLE I

CONTRACT NUMBERS FOR INVESTIGATORS

Investigator	Affiliation	JPL Contract
J. Lederberg, Proposal[a]	Stanford University	952489
E. Levinthal	Stanford University	952489
C. Sagan	Cornell University	952487
J. Pollack	Cornell University	952487
H. Masursky, Proposal[a]	U.S. Geological Survey	Defense Purchase Request (DPR) WO-8122
J. McCauley	U.S. Geological Survey	Defense Purchase Request (DPR) WO-8122
D. Wilhelms	U.S. Geological Survey	Defense Purchase Request (DPR) WO-8122
M. Carr	U.S. Geological Survey	Defense Purchase Request (DPR) WO-8122
D. Milton	U.S. Geological Survey	Defense Purchase Request (DPR) WO-8122
R. Wildey	U.S. Geological Survey	Defense Purchase Request (DPR) WO-8122
W. Borgeson	U.S. Geological Survey	Defense Purchase Request (DPR) WO-8122
R. Batson	U.S. Geological Survey	Defense Purchase Request (DPR) WO-8122
B. Smith,[b] P. I. Appointment 7/1/69	New Mexico State University	952488
B. Murray, Proposal[a]	California Institute of Technology	JPL/Campus Contract 69829, California Institute of Technology
M. Davies	Rand Corporation	500974
W. Hartmann	University of Arizona	952486
N. Horowitz	California Institute of Technology	JPL/Campus Contract 69829, California Institute of Technology
R. Leighton	California Institute of Technology	JPL/Campus Contract 69829, California Institute of Technology
C. Leovy	University of Washington	952491
T. McCord	Massachusetts Institute of Technology	952499
R. Sharp	California Institute of Technology	JPL/Campus Contract 69829, California Institute of Technology
W. Thompson, Proposal[a]	Bellcomm, Inc.	Supported by Office of Manned Space Flight, NASA; NASW-417
G. Briggs	Bellcomm, Inc.	Supported by Office of Manned Space Flight, NASA; NASW-417
P. Chandeysson	Bellcomm, Inc.	Supported by Office of Manned Space Flight, NASA; NASW-417
E. Shipley	Bellcomm, Inc.	Supported by Office of Manned Space Flight, NASA; NASW-417
G. de Vaucouleurs, Proposal[a]	University of Texas	952490

[a] Principal Investigators are under Jet Propulsion Laboratory subcontracts, originally sponsored by the National Aeronautics and Space Administration, under Contract NAS 7-100.

[b] Because of the pressure of other commitments, B. Murray was replaced by B. Smith on July 1, 1969.

3. *Extended Mission*

The nominal mission is designed for a duration of 90 days. However, various hardware modifications may make it possible to extend the lifetime of the spacecraft to a year or more. Increasing distance of the spacecraft and Mars from the Earth will then reduce the rate of data flow to the equivalent of only 50 to 100 pictures per month.

II. Organization

Operating relationships for the television experiment, showing the organization of the proposed investigators into a team effort, are discussed in the following paragraphs.

The Principal Investigators and Co-Investigators who submitted experiment proposals to use television imagery (see Table 1) were regrouped to function collectively as the Mariner Mars 1971 television team. The television team matrix is shown in Fig. 1. The team discipline or task group members were chosen from the investigators associated with the selected proposals.

Coordination of the television team efforts is performed by the team leader, who was named by NASA in consultation with the Principal Investigators in the area of television imagery. The team leader furnishes Project Management with recommendations concerning television equipment fabrication and modification, testing, calibration, mission operations

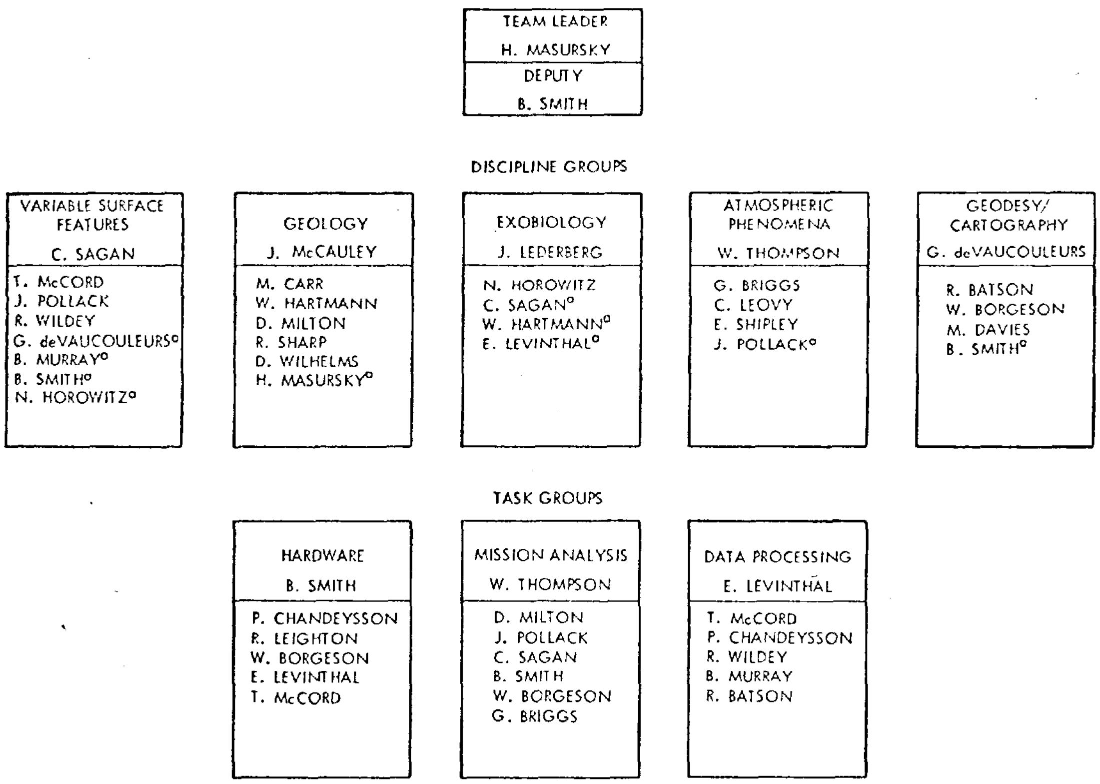

Note: The photointerpretation team matrix illustrates the current assignment of functions. This organizational structure will be reviewed by the Investigators periodically for adequacy to meet science and Project requirements. The organizational structure will be reviewed before receipt of the first Mars picture.

°Indicates second assignment.

Fig. 1. Photointerpretation team matrix.

(including orbital trajectory parameter selection), and image processing.

The team organization has been reviewed and altered several times since its original state. As new problems have arisen, new task groups have been formed to solve them. The hardware group was directed initially by Howard Friedman of the Jet Propulsion Laboratory, but was changed later to Bruce Murray. After Murray's appointment to the Venus-Mercury Program, he was replaced as chairman of the hardware group by Bradford Smith, who also replaced him as a Principal Investigator (on July 1, 1969). David Norris replaced Friedman in mid-1969 as the

(a)

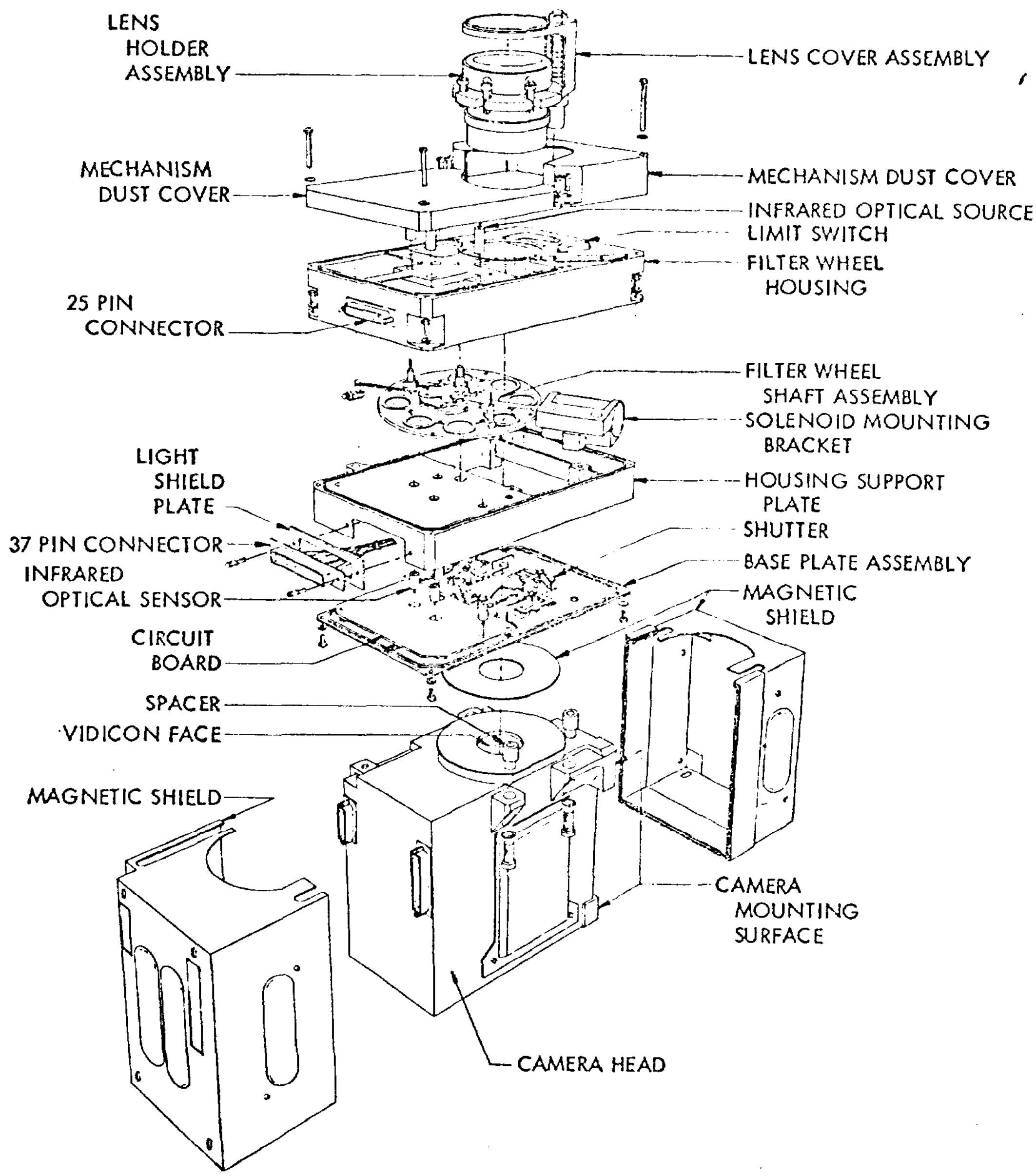

FIG. 2(a). Mariner Mars 1971 television subsystem: wide-angle camera.

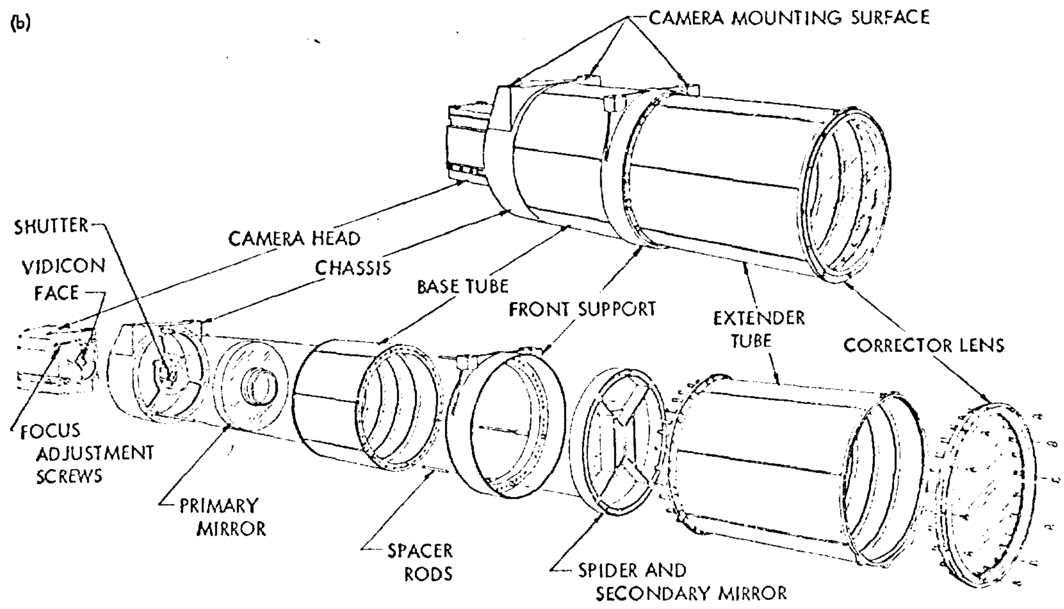

FIG. 2(b). Mariner Mars 1971 television subsystem: narrow-angle camera.

contact at the Laboratory for the hardware group.

III. INSTRUMENT DESCRIPTION

The television subsystem to be used in the Mariner Mars 1971 television experiment consists of two cameras (Fig. 2), which are mounted on the spacecraft planetary scan platform, with supporting electronics housed in the bus portion of the spacecraft. The wide- and narrow-angle optics and some portions of the electronics are identical to the equipment developed for the Mariner VI and VII television subsystem. (A simplified block diagram of one of the cameras is shown in Fig. 3.)

The wide-angle camera (50-mm focal length), which has a field of view of 11 by 14 deg, utilizes a six-element lens and is equipped with a filter wheel that can be commanded to place any one of eight

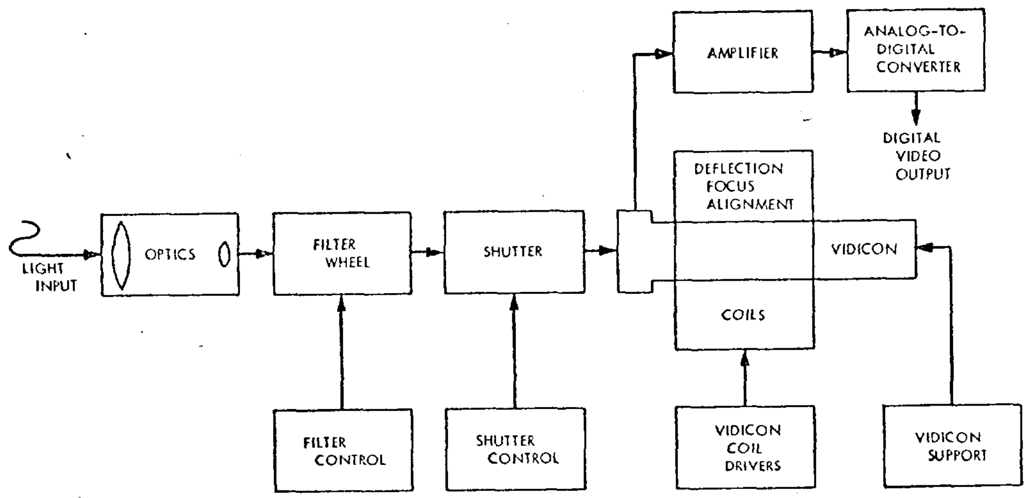

FIG. 3. Block diagram of slow-scan television subsystem.

TABLE II

TELEVISION CAMERA PERFORMANCE CHARACTERISTICS

Characteristic	Wide-angle camera	Narrow-angle camera
Focal length (mm)	50	500
Focal length ratio	$f/4.0$	$f/2.35$
Shutter speed range (msec)	3 to 6144	3 to 6144
Angular field of view (deg)	11 by 14	1.1 by 1.4
Active vidicon target raster (mm)	9.6 by 12.5	9.6 by 12.5
Number of vidicon reseau marks	111	111
Scan lines per frame	700	700
Frame time (sec)	42	42
Picture elements per line	832	832
Bits per picture element	9	9
Video carrier frequency (kHz)	28.8	28.8
Video baseband (kHz)	7.35	7.35
Video sampling frequency (kHz)	14.7	14.7
Video passband (kHz)	21.45 to 36.15	21.45 to 36.15
Resolution at 1800 km	1 km per picture element pair	0.1 km per picture element pair
Brightness range in automatic sequence (ft-Lamberts)		
High	2200 to 44	2200 to 44
Medium	1100 to 22	1100 to 22
Low	550 to 11	550 to 11

spectral and/or polarizing filters in the optical path. The wheel can be advanced zero, one, or two steps between consecutive wide-angle pictures by ground command, or will take two steps between each picture, cycling continuously through a four-filter sequence when in the automatic mode.

The narrow-angle camera (500-mm focal length), which has a field of view of 1.1 by 1.4 deg, utilizes a 200-mm-diameter Schmidt-Cassegrain telescope and the same type of video design as the wide-angle camera; it has a single fixed filter. The spectral range of the narrow-angle camera, therefore, must be established before launch.

Both cameras have focal-plane shutters, similar to the type used on the Surveyor and Mariner Mars 1969 television cameras. After passing through the filter and shutter, the optical image is focused onto a slow-scan vidicon, which is operated with a cathode-modulated electron beam. Vidicon electron beam focus, alignment, and vertical and horizontal deflection are performed magnetically. (See Table II for some of the significant instrument parameters.)

The video signal is processed by a video amplifier, as shown in Fig. 4. The modulated baseband video from the vidicon photocathode is current-amplified by a preamplifier (the maximum photocathode current is about 5 Namp), then bandpass-filtered, amplified, and refiltered. The signal is then demodulated, synchronous with the vidicon cathode chopping input. The demodulated video signal is amplified and low-pass-filtered to produce baseband video reconstruction, which is converted to a digital signal that forms 832 nine-bit words for each of the 700 television lines. The digital signal is transmitted to the data automation subsystem (DAS), where it is rate-buffered and formatted for input to the spacecraft's digital tape recorder. There it is stored until it can be played back, at a lower bit rate, to the Deep Space Stations and relayed to the Space Flight Operations Facility to be recorded and reconstructed into a picture. The 85-ft

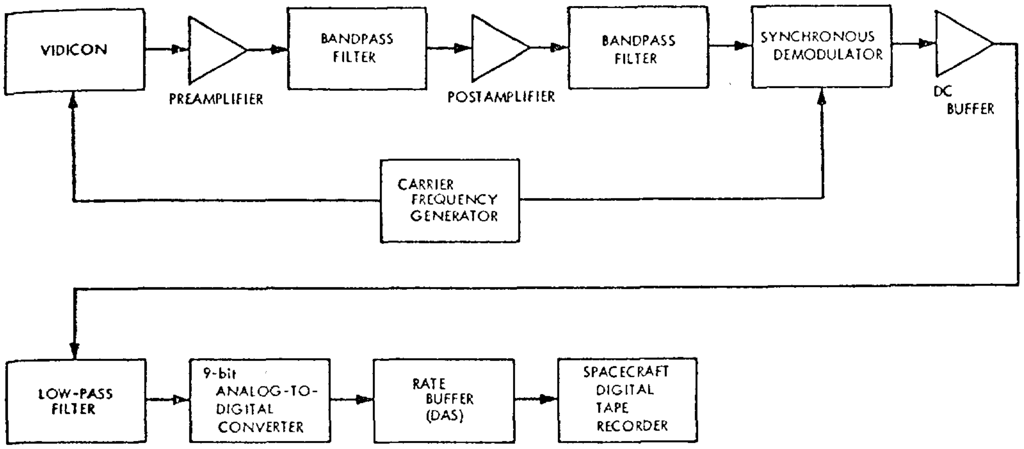

FIG. 4. Video signal processing.

antennas of the Deep Space Network are capable of receiving picture data, but at a much lower bit rate than the 210-ft antenna at Goldstone, California. Therefore, most picture playbacks must use the 210-ft antenna.

In addition to buffering the television data, the DAS supplies the various timing control functions for the television sweep circuits, and computes the average video levels of each wide- (or narrow-) angle picture to set the vidicon exposure time for the next wide- (or narrow-) angle picture.

The resolution of surface features and of the area in the field of view of each camera is dependent on the slant range from the cameras to the planetary surface. With the cameras pointed in the nadir direction and the spacecraft at an altitude of 1500 km, surface resolution in the wide- and narrow-angle cameras corresponds to about 1 and 0.1 km, respectively. The definition of resolution used here is described below.

It is possible, by ground command, to take one single wide- or narrow-angle picture, to take pictures in wide- and narrow-angle pairs at selected points on the surface, or to take a mixed sequence (wide, narrow, narrow, wide, etc.) of pictures until the tape recorder is filled (about 32 pictures). In the automatic-exposure-control mode (no use of an overriding ground command), the television pictures will be recorded in a continuous alternating camera sequence. In this mode, there are three brightness ranges, which are the same for both cameras, giving a total brightness range of from 11 to 2200 ft-Lamberts.

IV. INVESTIGATIONS

The television experiment on Mariner Mars 1971 consists of two distinctly different, but complementary, types of investigations, one of which will be assigned to each of the two spacecraft. The first, which is called the fixed-features investigation, serves a wide range of basic data needs and is designed principally to define the geology and topography of Mars at resolutions consistent with broad, contiguous coverage. This investigation can be conducted most efficiently by a 12-hr Goldstone-synchronous orbit of high inclination (50 to 80 deg) with periapsis initially about 15 deg from the terminator (see Fig. 5). The second and more complex mission, called the variable-features investigation, is concerned primarily with the detailed study of diurnal, seasonal, and secular variations, including surface and atmospheric phenomena. The variable-features investigation can be conducted most efficiently by an orbital period of 32.8 hr, a 4/3 harmonic of the planet's rotational period—with periapsis chosen to lie either near the terminator or the

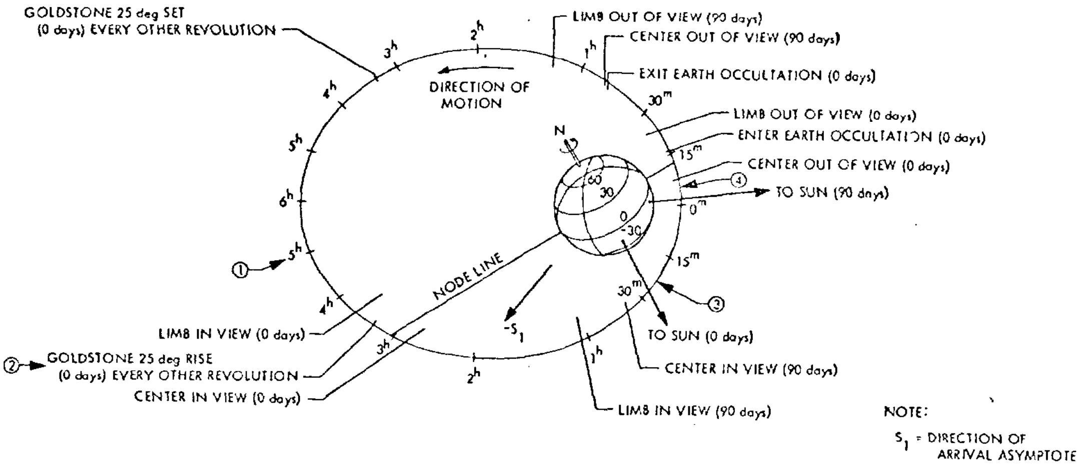

FIG. 5. Mariner Mars 1971 12-hr mapping orbit.

subsolar longitude, depending upon a further weighting of mission objectives (see Fig. 6). The inclination is to be as low as possible, while still avoiding Sun occultation (probably 40 to 50 deg).

Although primary responsibility for the fixed-feature and variable-feature investigations will be assigned to Missions A and B, respectively, it is reasonable to assume that both spacecraft will contribute to both types of studies. Contingency plans, in the event of failure of one spacecraft before or after insertion, have yet to be developed; there is general agreement that both types of data are essential to obtain the maximum potential of the 1971 missions.

1. *Fixed Features*

Scientific Objectives

A requirement for systematic scientific exploration of a solid heterogeneous planet is the detailed knowledge of its surface. Therefore, the principal objective of this mission is to acquire the maximum amount of geologic, geodetic, topographic, and cartographic data at the most useful resolutions. These data will permit study of surface distribution of bright and dark regions, fine structure of minor topographic

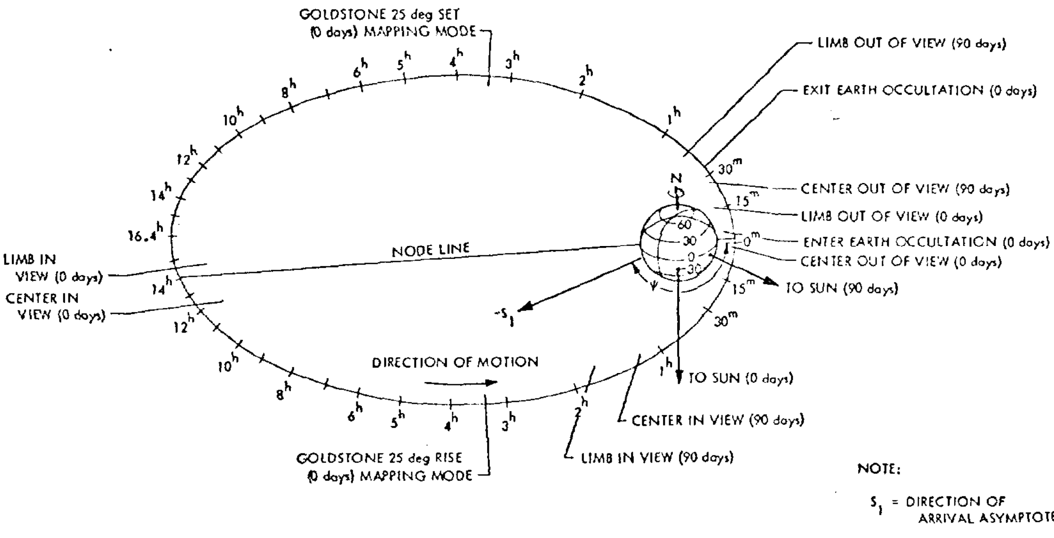

FIG. 6. Mariner Mars 1971 32.8-hr variable features orbit.

details, and analyses of processes such as volcanism, tectonism, impact, mass wasting, and aeolian activity, thus greatly improving knowledge concerning the structure and evolution of Mars as a planet.

Geometric and photometric optical imagery of the surface of Mars will permit the following:

(1) A determination of the shape or figure of the planet, i.e., the ellipticity of the mean surface reference level which may differ from the dynamic ellipticity (as suggested by Earth-based data); this, in turn, will provide information on possible departures of the planet from hydrostatic equilibrium, which may be supported by stresses in the upper crust.

(2) The derivation of high-precision geodetic coordinates of a large number of well-defined topographic features necessary to construct greatly improved maps of the planet, i.e., charts of the surface distributions of albedo and elevations in a rigorously defined geodetic network; it already is evident from Earth-based radar data that albedo and elevation differences on Mars do not have a close correlation. Detailed studies of this correlation (or lack of it) may have great significance for an interpretation of observed albedo variations.

(3) A synoptic geologic and topographic map of Mars at the largest practical scale, based on interpretations of low and high Sun angle imagery, will be compiled.

(4) Enhancement of the interpretability of the variable-features investigation. The degree of topographic dependence is one of the most important questions regarding the wave of darkening. This can be determined only by pairing the high Sun albedo variation data of the variable-features investigation with the low Sun topographic data of the fixed-features investigation.

(5) Construction of a framework to interpret the data from the other experiments concerned with surface properties or bulk characteristics (infrared radiometry, infrared spectroscopy, S-band occultation, and celestial mechanics experiments are obvious examples). Lunar mascons suggest that there may be gravity variations relatable to the surface structure.

(6) Effective planning for high-resolution orbiters and landers throughout the 1970s. The Mariner Mars 1971 fixed-features investigation will provide broad, contiguous photographic coverage at uniform resolution that will be similar to the Earth-based lunar telescopic photography, along with nested spot samples at 10 times greater resolution. It will, like the lunar photography, provide a comprehensive, and therefore flexible, decision-making base for future exploration efforts.

Visual Resolution and Its Operational Implications

The Mariner Mars 1971 television subsystem was inherited without substantial modification from earlier flyby missions. Its maximum resolution capability is somewhat less than that considered optimum for planetwide reconnaissance, primarily because of limitations in the optical system, the lack of image motion compensation, and the necessity to keep a high periapsis in order to maintain planetary quarantine restrictions. If, however, the system operates at or near its resolution limits, a very meaningful regional reconnaissance can be conducted. To achieve this goal, the photographic coverage must be obtained within a narrow range of illumination conditions, i.e., at low Sun angles, in order to increase target contrast and thus maximize photographic resolution.

The term resolution, as it is applied to television experiments, often leads to confusion about true system capability. To avoid this difficulty with regard to the Mariner Mars 1971 flights, a brief discussion of resolution as it applies to television experiments is presented in the following paragraphs.

Photographic resolution is usually stated in terms of separable white-on-black line pairs per millimeter in the image. In spacecraft vidicon systems, the scale width of a single television line at a particular altitude is often given as the index to system resolution. The value for the width of a television line of the wide-angle

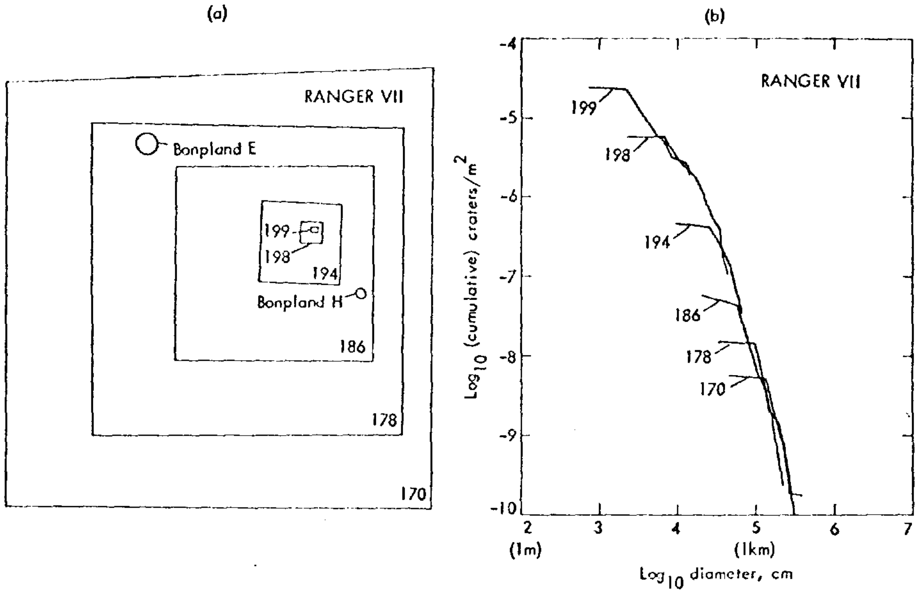

FIG. 7. (a) Areal coverage of selected, nested Ranger VII frames. (b) Cumulative crater frequency plots from frames indicated.

camera for Mariner Mars 1971, from a periapsis altitude of 1500 km, is $\frac{1}{2}$ km. This does not mean, however, that one can actually recognize $\frac{1}{2}$-km objects on the surface. For any given spacecraft television subsystem, the size of the smallest recognizable object is a function of overall target contrast, which is highly dependent on Sun elevation, shape, sharpness of outline, and other factors. For example, high-contrast objects such as fresh, young craters are more detectable than subdued, older craters. The more numerous small, subdued craters of an impact population cannot be seen near the resolution limit; however, small, sharp craters of the same size are readily detectable. The observed size–frequency distribution is thus censored as it approaches the resolution limit of the system; cumulative crater counts usually show a "roll-over," or flattening, at about 4 to 6 times the size of the smallest identifiable crater. This effect can be seen in Fig. 7 from the unpublished terrain analysis work by Edgar Bailey, U.S. Geological Survey, who prepared cumulative crater counts from single, nested, progressively higher resolution Ranger VII frames. The cumulative plot for each individual frame shows this roll-over at a point about 5 times the size of the smallest detectable crater. The widely cited roll-over of the Mariner IV crater frequency curve below 20 km and the "genuinely lower abundance and/or systematic change to smoother craters on Mars" (Sharp *et al.*, 1967), at a point about 5 times the size of the smallest detectable crater, can be looked upon with some suspicion (Chapman *et al.*, 1969). This roll-over may, in fact, not reflect any fundamental change in surface characteristics in the vicinity of 20 km, but simply may reflect an overestimate of the real identification resolution of the Mariner IV television subsystem.

Extrapolation of the Mariner IV curve to 1 km produces a crater deficiency almost an order of magnitude below the number actually measured in the Mariner VI high-resolution narrow-angle pictures (Leighton *et al.*, 1969). Similar effects produced by resolution falloff in the small size ranges can be anticipated for the Mariner Mars 1971 cameras so that the real resolution will be much less than the figure given for the scale width of a single television line.

The effect of lighting angle on resolution has important operational implications.

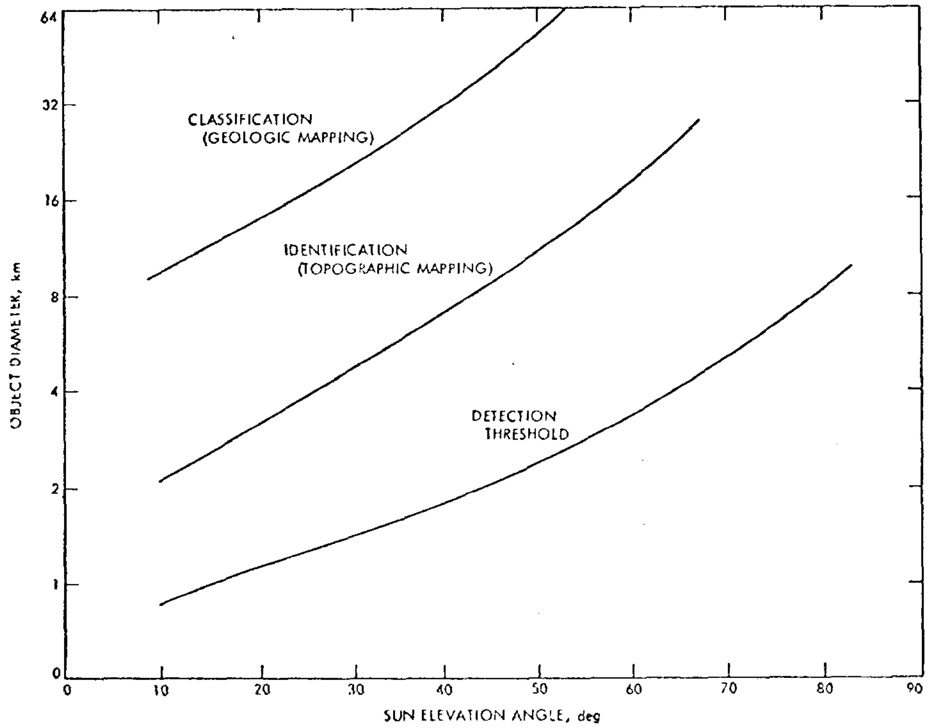

FIG. 8. Relationship between types of resolution and Sun elevations. (After Keene, 1965.)

Keene (1965), in an empirical study before the first Lunar Orbiter flight, was able to determine quantitatively the effect of variation of lighting angle on the resolution of a photographic subsystem. Objects of varying size and shape, with reflectance properties similar to those of the Moon, were photographed at varying Sun elevations; the response by viewers was categorized into zones of no detection, detection, and identification as a function of object size and Sun elevation. Figure 8 is an adaptation of Keene's general results which, in spite of limited knowledge of the Martian photometric function and large-scale topography, are parametrically applicable to photography of Mars.

Three positively sloping curves define the different types of resolution important in a television experiment. The first is detection resolution, which is the zone in which the presence of an object can be established in the image, but the object cannot be classified. If, for a given system, the detection resolution at a Sun elevation of 10 deg is taken as about 1 km (at a height of 1500 km, the detection resolution of the Mariner Mars 1971 wide-angle camera will be about 1.5 km), then the effects of increasing lighting angle can be assessed. At a Sun elevation of 50 deg, the detection resolution falls off by about a factor of 2. Thus, detectability is at a maximum near the terminator because of the enhanced contrast produced by shadows, and it decreases with higher illumination. The second curve defines the zone of identification resolution in which one can discriminate between topographic forms such as hills, peaks, craters, etc., but in which thorough photogeologic analysis is not practical. The classification, or geologic mapping curve, has been added to Keene's plot by comparison of the smallest objects mapped by the U.S. Geological Survey to the detection resolutions of the Ranger and Lunar Orbiter spacecraft. In general, there is almost an order of magnitude difference between the standard detection resolution and the size of the smallest geologically classified feature, irrespective of variation in Sun angle. Thus, a 1-km feature may be detectable at a Sun elevation of 10 deg, but a feature must be about 4 km across to be truly recognizable, and at least 8 to 10 km before it can be classified in a geologic sense.

Figure 8 shows the importance of near-terminator periapsis photography for the fixed-features investigation. If the television experiment is to yield topographic data to the limit of its restricted capabilities, most of the imagery should be acquired at Sun elevations no greater than 30 deg because of resolution falloff. Preliminary evaluation of the Mariner VI and VII pictures indicates that the near-terminator region is photographable. No obvious veiling atmospheric haze or obscuring cloud cover were detected in the semi-vertical near-encounter pictures (Leighton *et al.*, 1969). The information content of the pictures, except for the very bland terrain in the floor of Hellas, is good up to illumination angles of 30 deg. Topographic details can be discerned at angles of 60 to 70 deg in the case of "chaotic" terrains. Thus, most of the Mariner Mars 1971 fixed-feature coverage can be programmed for Sun elevations between 10 and 30 deg, but the capability will exist to acquire higher Sun angle data in the event of temporary atmospheric problems or for special purposes such as the acquisition of albedo data.

Mission Profile

The nominal 12-hr mapping orbit is shown to scale in Fig. 5; viewing conditions at the beginning and end of the 90 days in orbit are indicated. A mapping sequence begins with Goldstone rise about 5 hr before periapsis passage (1). When the Goldstone elevation angle reaches 20 to 25 deg, the spacecraft will empty the tape recorder of the television data taken during the previous periapsis passage when Goldstone was at the antipode (2). The readout takes about 3 hr when the 16.2-kbps data rate is used with the 210-ft Goldstone antenna. When the recorder is playing back, no other science data can be transmitted. About 20 min before periapsis (3), the television camera begins to take pictures which are sent to the now-empty tape recorder for storage. The other instruments send their data simultaneously to the tape recorder while transmitting it back to Goldstone in real time. The picture-taking sequence ends a few minutes after periapsis passage, when the tape recorder is full and the spacecraft is approaching the dark side of the planet (4). Occasional observations of Phobos and Deimos (and Saturn for calibration purposes) may be obtained between (4) and (1), and at other orbital positions.

Because the orbital period is 12 hr and the rotation rate of Mars is about 24 hr 37 min, the planet will rotate slightly less than 180 deg per orbital revolution. Thus, mapping coverage of alternate sides of the planet will be coupled with a small (about 9 to 10 deg) daily shift in longitude of the subperiapsis point (Fig. 5). A complete mapping circuit in an eastward direction around the planet will be completed in about 20 days. After 90 days, the area between −60 and +40 deg latitude will have been covered by the wide- and narrow-angle cameras: the wide-angle camera, with contiguous, low-resolution ($\frac{1}{2}$ km/television line) pictures, and the narrow-angle camera with uniformly interspersed spot coverage at higher resolution (50 m/television line). The area covered during each 20 days, and typical "footprints" for the wide-angle camera coverage are shown in Fig. 9. Regions of special interest can be re-examined every 20 days with a full array of sensors. Thus, during the mapping phase, there will be opportunity for adaptive operations, making use of previously recorded data. Barring severe equipment problems, however, the fixed-features investigation should proceed in a more systematic and less adaptive fashion than the variable-features investigation.

After 20 to 54 days in orbit, depending on the actual performance of the high-rate channel, the sequence will be modified because increasing Earth–Mars distance will cause the tape playback rate to be dropped to 8.1 kbps, even with the use of the 210-ft antenna. At that time, either a full tape recorder of data will be taken at

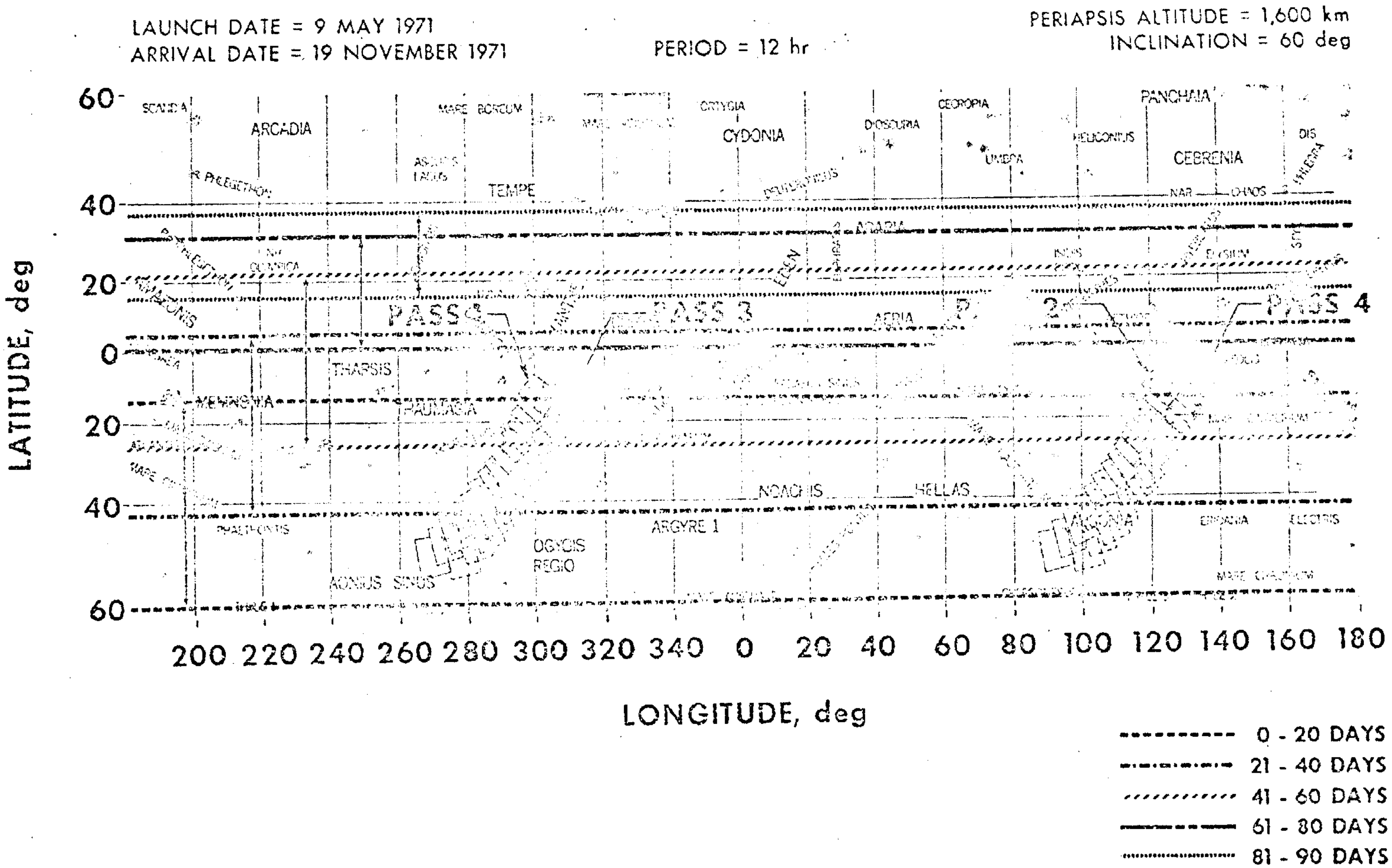

FIG. 9. Areal coverage and typical wide-angle camera footprints for 12-hr orbit of 90-day mission.

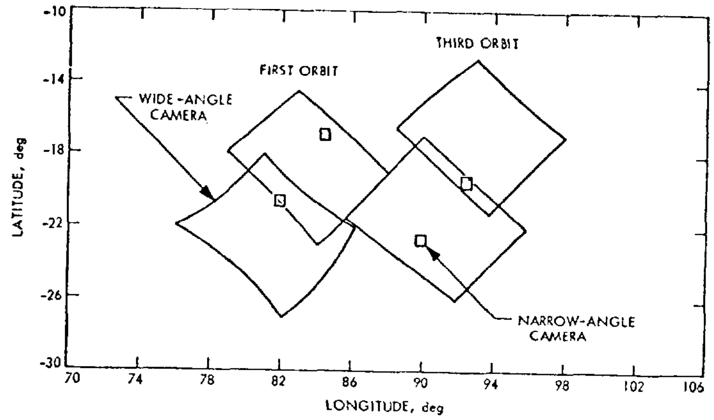

FIG. 10. Relationship of narrow-angle camera coverage to wide-angle camera footprints.

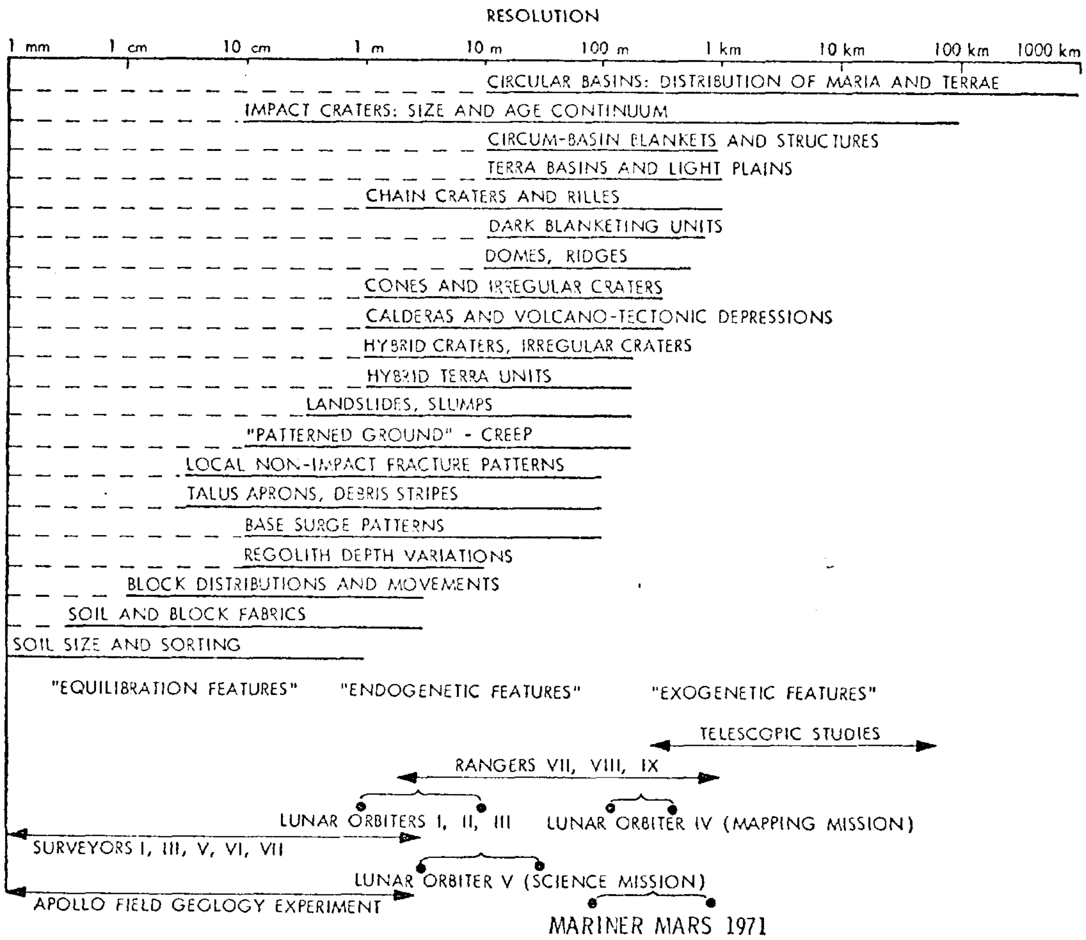

FIG. 11. Resolution thresholds and points of diminishing information returns for selected lunar features.

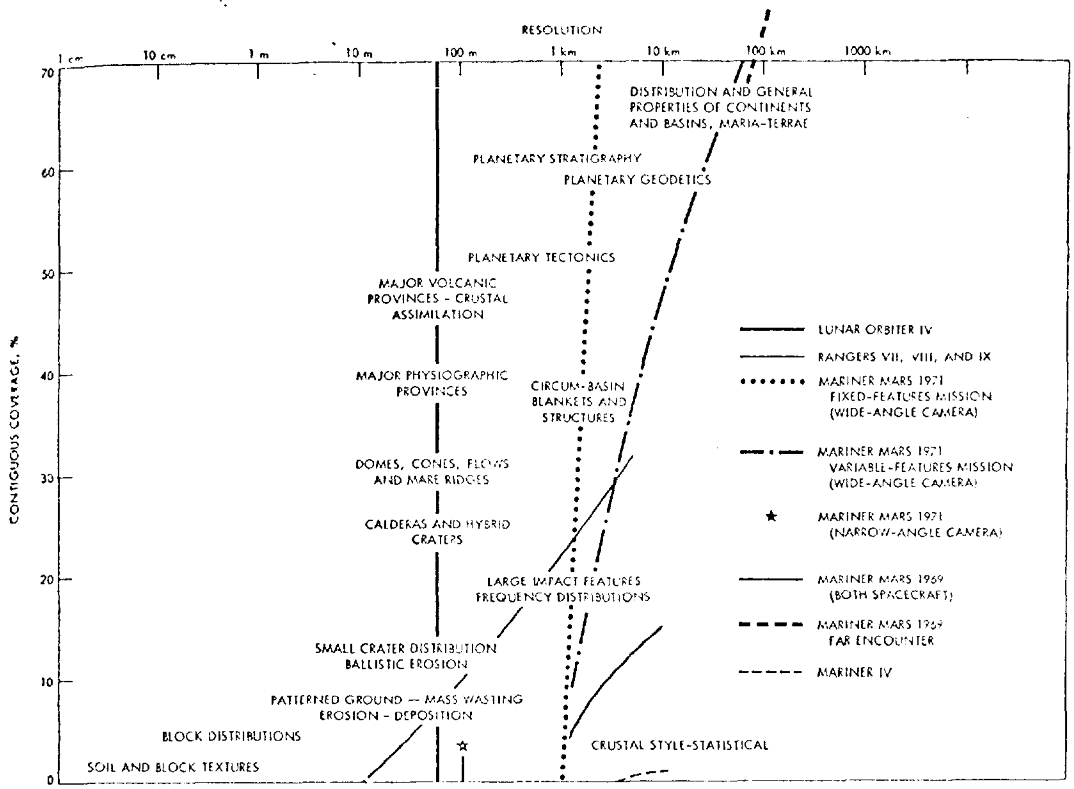

FIG. 12. Comparison of Mariner Mars 1971 fixed-features investigation with performances from other spacecraft.

every other periapsis or half the amount of data will be taken at each periapsis passage. The rest of the sequence stays the same. There is considerable overlap in the coverage from each 20-day longitudinal cycle. This characteristic is particularly advantageous in the fixed-features investigation because it gives the capability of acquiring, in these zones of overlap, either pictures taken with high Sun angles, convergent stereo (explained later), or special-purpose color and polarimetric data without sacrificing contiguous coverage.

Figure 10 shows the area covered by the narrow-angle camera in the "footprint" of the wide-angle camera. Although almost 70% of the planet will be covered by the 1.0-km-resolution wide-angle camera, about 5% will be covered by the 0.1-km-resolution narrow-angle camera. This small fraction of the surface sampled at a tenfold gain in resolution, however, will allow observation of many features of fundamental geologic, geophysical, and geochemical importance (Figs. 11 and 12). If features of exceptional interest are observed, narrow-angle pictures can scan the region of these features in later passes, and convergent high-resolution stereo coverage can be obtained at the sacrifice of systematic wide-angle coverage.

Anticipated Results

Geodesy. The basic element for the exploration and mapping of the surface of a planet is the three-dimensional shape of this surface, i.e., the "figure" of the planet. In a fast-rotating planet such as Mars, the normal expectation is that the surface is very nearly in approximate hydrostatic equilibrium under the combined effects of centrifugal force and gravity, allowing for the internal mass distribution. A persistent discrepancy between the dynamic ellipticity derived from perturbations of the satellite orbits (and more recently the earlier Mariner flights) ($f_d = 0.00525$) and the optical ellipticity of the disk derived from many consistent visual and photographic observations ($f_o = 0.0105$; de Vaucouleurs, 1964) has been frequently discussed in the past and remains unexplained. A combined analysis of the limb contour from preinsertion and apoapsis photography and a new geodetic control network should lead to a definitive solution for the average shape of the Martian surface. Such a study is also needed to define the Martian equivalent of the geoid, i.e., a standard reference surface for mapping. Departures of the actual surface from the reference spheroid will give information on elevations and, in conjunction with gravity studies, on departures from hydrostatic equilibrium and isostasy. A refinement of the direction of the rotation axis of Mars, currently known to a precision of about 0.1 deg, will also follow from an analysis of the apparent motion of the control points on the surface due to planetary rotation.

Cartography. A primary objective of the Mariner Mars 1971 missions is an accurate mapping of albedo and a new geodetic control network to determine the physical size and shape of the planet and to solve for the direction of its spin axis. This network of points on the surface of Mars also is used to orient the planetwide coordinate system for the preparation of cartographic materials. The control points are identified on a series of different pictures and their positions measured; then, by analytical triangulation, their coordinates on Mars can be computed using the spacecraft's known locations on its trajectory. Once the locations of the control points are known, it is possible to solve for spacecraft positions at which additional pictures have been taken by these same photogrammetric techniques. In this way, the Mariner VI and VII pictures will be used to define a control network for positioning the topographic detail and markings on the new charts of Mars.

It will be possible, for several reasons, to use the Mariner Mars 1971 pictures to improve the accuracy of the Martian geodetic network. The most important reason is the flexibility of picture-taking with regard to altitude and coverage permitted with the long-duration orbital flight in contrast to the flyby missions. Thus, it will be possible to obtain high-resolution pictures of most of the planet for detailed identification of the control points as well as at a more optimum altitude for making measurements. Wide-angle pictures taken between 7000- and 14000-km altitude collectively covering the entire surface of Mars should be a good compromise of resolution and area covered for locating and measuring the positions of control points. The camera positions on orbit in 1971 should be known with greater precision than could be determined after the 1969 flyby when uncertain outgassing shortly before encounter artificially modified the trajectory. Improved camera calibration and the increased number of reseau marks should also improve the 1971 measurements over those obtained in 1969.

Discrepancies of 5 to 10 deg in latitudes and longitudes (300 to 600 km at the surface) are not uncommon between various published maps (de Vaucouleurs, 1963); a recently completed 10-year Mars Map Project (de Vaucouleurs, 1970) in which all Earth-based visual and photographic data from 1877 to 1958 were rigorously reanalyzed and reduced to a common system of geodetic coordinates may have reduced errors to about 1 deg or a little better (~50 km), at least in regions where sufficiently well defined and stable surface "markings" (i.e., albedo variations) are available at ground resolutions varying from ½ to 1 deg ≃ 30 to 60 km in high-contrast regions to perhaps 2 to 3 deg ≃ 150 km in low-contrast regions. One of the major mapping applications of the high- and low-Sun wide-angle camera photography will be to locate precisely, in a well-defined geodetic coordinate system, the surface distribution of albedo differences and to compare it with surface elevation differences to a resolution limit of 1 or 2 km.

Topography. The major initial product from the fixed-features investigation will be contiguous (forward and side lapping) low-Sun-angle imagery of about 70% of the planet. In these pictures, surface textural detail will be emphasized at the expense of detailed albedo variation data. However, high-Sun-angle pictures of selected areas will be acquired in the zones of overlap shown in Fig. 10 and also from the variable-features investigation. If the first spacecraft performs nominally for 90 days, the wide-angle camera should provide about 2500 individual pictures at a detection resolution on the order of 1 km. The narrow-angle camera will provide the same number of nested, noncontiguous pictures with detection resolution of about 100 m.

Hypsometric control for cartographic purposes will be weak because of the limited stereometric capability of narrow-angle, small-format, high-altitude orbiters (Borgeson, 1966). In the nominal stereo mode (50% forward lap), the ΔH or height-measuring capability of the wide-angle camera will be on the order of 3 km. If operated in a convergent stereo mode,[2] ΔH can be improved to better than 1 km. Because this operation will create undesirable gaps in the mapping coverage, it will be used only in special-interest situations, probably in the zones of overlap between 20-day longitudinal cycles (see Fig. 9). Most of the relative height data from this mission will be derived, as in the lunar telescopic case, from shadow-length measurements with an estimated precision on the order of 200 to 1000 m. This relief measurement technique requires low-Sun, near-terminator conditions in order to have an acceptable percentage of the total area of each picture in shadow. This represents a second justification for near-terminator operations.

Keene (1965) gives a plot that is useful in estimating the percentage of area in shadow for surfaces of varying roughness under different lighting conditions. If the 1-km scale, depth-to-diameter ratios on Mars are on the order of 0.05 (5.7 deg), as suggested by Mariner IV photometric data, the shadowed area should be less than 1% of each picture at a Sun angle of 25 deg. At 15 deg from the terminator, however, the shadowed area increases to about 70%, an acceptable figure for shadow measuring. Although this technique can provide an abundance of high-quality, relative relief data, it will not be useful for the production of contoured maps. The main products from the visual imagery probably will consist of orthophotographic mosaics and semiquantitative airbrush renditions of the surface, with local spot elevations from the shadow-length measurements similar to the 1:1000000-scale lunar charts prepared from telescopic data by the Aeronautical Chart and Information Center.

An additional monoscopic slope-measuring technique called "photoclinometry" can be used for supplemental relief information. However, the technique is dependent on low-Sun and near-full-phase pictures of the same area at similar resolutions to control albedo effects, and on an accurate photometric function. In the lunar telescopic case, even with a well-described photometric function, a small error in albedo correction can lead to as much as a 100% error in slope determination (Rowan *et al.*, in press). Where the albedo is not constant, as on Mars, the problem of extracting truly meaningful slope measurements becomes almost insurmountable. Another aspect still under investigation for the Moon, is that photoclinometric profiles at comparable scales generally give lower roughness values than those derived photogrammetrically. It is theoretically possible, however, to tie together the photogrammetric and photoclinometric profiles to achieve better results than can be obtained singly by either method, but the methods are time-consuming and expensive (Wu, 1969).

Although considerable emphasis has been placed on this technique in past and present unmanned flight programs,

[2] Principal point at center of successive frames by means of fore and aft or sideways tilt along the orbital path.

particularly for Apollo site evaluation, it should be considered as a supplemental method of extracting relief data. The primary value, when used by itself, is in the statistical evaluation of the relative roughness characteristics of terrain units for geologic classification and for engineering purposes (Rowan *et al.*, in press) and in estimating the shapes of objects such as boulders and their tracks near the limiting resolution of an imaging system.

Geology. One principal geologic result of the fixed-features investigation will be a synoptic map of Mars at the largest practical scale, with emphasis on regional structure and stratigraphy. At the present time, 1:5000000 seems to be the most practical scale for the planned coverage; in this case, the map should resemble, in degree of detail, Earth-based lunar geologic maps (Wilhelms, 1969). This type of classification work has extensive terrestrial and lunar precedent and has proved to be an effective and reproducible analytical method. It does require, however, qualitative experience-based judgments with regard to the relative importance of various textural criteria for classification purposes. A unique characteristic of the geologic mapping approach is the use of observable superposition, intersection, and embayment relations in the reconstruction of surface history, thereby introducing time into the analysis. A further asset is that geologic mapping forces treatment of the visual and other data from the entire electromagnetic spectrum in an internally consistent manner. Observation is separated from interpretation; thus, special genetic pleas based on previous theory and partial treatment of the available data are, for the most part, avoided. A rock-stratigraphic approach will be used, based on that long applied terrestrially, and introduced in systematic geologic mapping of the Moon in 1961 (Shoemaker and Hackman, 1962; McCauley, 1967), and more recently adopted in the Soviet Union by Sukhanov, Trifonov, and Florensky, and in Great Britain by Guest and Murray.

Reduction of remote sensing data to the form of meaningful planetwide geologic maps requires that there be an effective tradeoff between the resolution that the system is capable of delivering and the amount of coverage obtained to be sure that major landforms are properly sampled and that they can be spatially related to one another. The solution of the tradeoff lies in the nature of the planetary surface in question and the scales at which various phenomena can be studied.

The importance of object scale in attempting to understand or to model terrestrial geotectonic phenomena has been described by Carey (1962). The scale dependence of observation, experiment, and theory is implicit in most work in terrestrial geology; but this fact is often overlooked. Studies of the Moon by telescope and by unmanned probes (Ranger, Lunar Orbiter, and Surveyor) that spanned some six orders of magnitude in resolution capability revealed a scale dependence or hierarchy of surface forms like that described for the Earth by Carey (see Fig. 11).

Selected examples of the types of features recognized are plotted; the beginning of the bar at the right indicates the detection resolution or scale at which one begins to acquire useful visual information for the particular feature. The dashed segments of the bar at the left indicate the scale range in which high-resolution data are, for the most part, unnecessary. The beginning of the dashed line could be considered as the point of diminishing returns or the point at which it is no longer reasonable to attempt high-resolution photography at the expense of coverage that could be used more profitably elsewhere. A point of maximum efficiency in a given experiment, i.e., where the most effective tradeoff between resolution and coverage is achieved, can be defined and lies near the center of each solid bar.

Figure 11 also indicates that there are certain critical-resolution thresholds for the Moon, marked by the beginning points of each bar, to the right of which (low-resolutions) the data are insufficient for effective geologic analysis, the amount of coverage obtained notwithstanding. As an example, at 1-km resolution in the telescopic range, one can do a respectable job with gross lunar exogenetic features, e.g., the circular basins and large impact craters. High-resolution data from the various imaging probes were necessary, however, to deal effectively with the naturally smaller-scale features of internal origin, e.g., volcanic, tectonic, and mass-wasting phenomena (endogenetic and equilibration features). A similar set of critical-resolution thresholds for Martian landforms can be expected, and several examples can be seen in the data from Mariners VI and VII. Most of the Mariner VI wide-angle camera coverage in near-encounter sequence (Frames 17, 19, 21, 23) with resolutions on the order of 1 km per television line shows only flat-floored, almost rimless craters surrounded by what appears to be featureless terrain (Fig. 13). The nested narrow-angle pictures (Frames 18, 20, 22) with resolutions of about 0.1 km per television line, on the other hand, show that gentle linear ridges and patches of blocky terrain are present locally, indicating that the inter-crater areas at higher resolution are actually more complex than they appear in the wide-angle camera. Another resolution threshold crossed by the narrow-angle camera is evidenced by the change in frequency of sharp appearing craters in narrow-angle pictures, as opposed to those observed by the wide-angle camera (Leighton *et al.*, 1969).

In addition to imagery well below the threshold necessary for assessment of the relative roles of internal and external processes, the other special requirement for effective geologic analysis is that the coverage be contiguous and at uniform resolution. This stems from the requirement for a regional setting for each geologically classified feature. The advantage of recognizing a field of small, irregular craters is doubtful unless it is known whether they are part of a field of similar craters that surround a single, much larger crater. If one has the coverage to establish this fact, the small, irregular craters may be identified from their spatial distribution as secondaries. Uniform resolution demands that the pictures be taken at about the same place in the orbit (near periapsis) and with approximately the same lighting. The need for reasonably uniform resolution is derived from the internal consistency requirement in geologic mapping. If a unit is defined and outlined on the basis of fine textural properties, cumulative crater frequency or any other morphologic characteristic, the resolution must remain reasonably constant throughout the study area if the boundaries and relations to other units are to be effectively defined.

Crater Studies. With detailed photography of a substantial portion of Mars, we can make advances in several areas that bear on the ancient meteoroid environment of Mars and on surface processes during its history: (1) Detailed structure of the largest Martian basins and their similarity to the multiring lunar basins may shed light on both Martian and lunar features. Are the lunar basins low-velocity impact sites involving circumterrestrial bolides unique to the Earth-Moon system? (2) If uneroded, preserved cratered areas can be identified on Mars, are the densities and sizes of craters compatible with the numbers and lifetimes of Mars-crossing asteroids? (3) Are there ancient regions saturated with craters, or are the oldest regions unsaturated? (4) Do small-scale structures systematically show features indicative of erosion processes? How have craters been erased in the craterless areas such as Hellas?

Relation of Fixed-Features Investigation to Earlier Television Experiments

Figure 12 is an attempt to relate the mapping phase of the fixed-features investigation to the results of other unmanned probes and to a nominal variable-features investigation in order to contrast the operational styles of the two types of investigations and to show, in terms of a better geologic understanding of Mars, what is expected from the mapping phase of the investigation. Fifteen types of planetary investigations, identified from available literature concerning the Moon and Mars, are positioned approximately in terms of the resolution required and

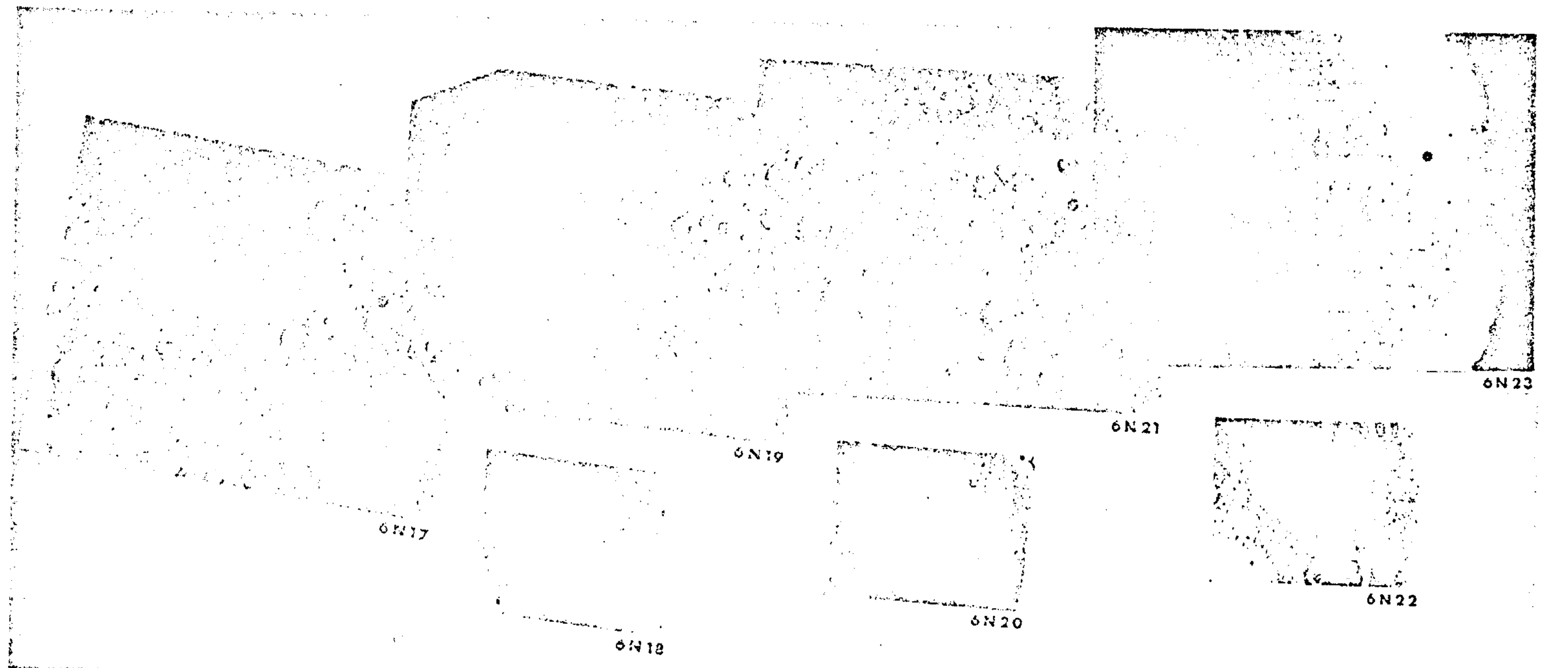

FIG. 13. Mosaic of selected Mariner VI pictures from wide- and narrow-angle cameras (wide-angle camera resolution: about 1 km/TV line. narrow-angle camera resolution: about 0.1 km/TV line). Pictures are of the Deucalionis Regio area. The terminator is at the far right; north is at the top. The east–west dimension of the narrow-angle camera strip is about 3600 km. Note the complexity of the terrain in narrow-angle picture 6N22.

estimates of the amount of contiguous coverage necessary to study the particular phenomenon and to place it in a regional context. The lines shown for each mission define a zone (to the right of each line) in which the studies identified can be conducted meaningfully. Studies that are shown to the left of the lines are not possible, because resolution is below the required threshold. It can be seen that the Mariner IV, VI, and VII missions permit only generalized studies of the surface structure of Mars and, perhaps, some preliminary work on large crater frequency distributions hampered both by resolution and coverage limitations. The Mariner VI and VII far-encounter sequences and the polar cap coverage represent advances over Mariner IV.

The coverage of the mapping mission by the wide-angle camera on Mariner Mars 1971 should be better by a factor of 2 than the coverage by the wide-angle camera on Mariners VI and VII and similar in information content to the lunar telescopic data, thus permitting the same type of regional, structural, and stratigraphic analyses performed before Ranger and Lunar Orbiter. The narrow-angle camera enhances overall mission potential with its spot-sampling capability and may permit study, on a statistical basis, of some phenomena that fall in the Lunar Orbiter IV range—secondary craters and internal features. An additional asset is the ability to point the narrow-angle camera, without sacrificing contiguous coverage, at areas previously determined to be of special interest in the zones of redundancy.

The Mariner VI and VII television results support the current plan for two complementary missions in 1971. Although apparently smoother and less cratered at comparable photographic scales (1 km and 0.1 km per television line) than some parts of the Moon, Mars presents, with the exception of the floor of Hellas, a moderately variegated surface on which at least four major types of terrain can now be recognized. The data from Mariners IV, VI, and VII suggest that it is a primitive body more like the Moon than the Earth, but that it probably is of comparable geologic complexity. In the case of the Moon, some 44 major rock-stratigraphic units and 10 different geologic provinces are now recognized on the near-side (Wilhelms and McCauley, 1969). The distributional patterns of these units are the key to unraveling surface history. With the improved resolution expected from the Mariner Mars 1971 television subsystem, the recognition of additional terrain units can be anticipated and the distribution patterns of these will be delineated by means of the contiguous Mission A coverage. This then will be the framework within which to interpret data on variable features and to plan subsequent investigations, particularly surface sampling by landers such as those envisioned for 1975.

2. *Variable Features*

Mariner Mars 1971 will provide the first opportunity to study features of the surface and characteristics of the atmosphere of the planet with good spatial and temporal resolution—a significant advantage, since diurnal, seasonal, and secular variations are widespread on Mars, and since fine topographic structure has been detected. The phenomena of interest are of considerable meteorological, geophysical, and exobiological importance. They include the seasonal and secular contrast and reflectivity changes of dark areas; possible seasonal changes in the opposite sense in bright areas; secular changes in the boundaries of dark areas; recession of the polar cap, the vertical structure, together with spatial and temporal variations, of the gaseous atmosphere and any hazes associated with it; yellow and white clouds; and surface frost patches. These phenomena are discussed in the following paragraphs. In addition, it is important to determine locales where significant seasonal or other variations occur to aid landing site selection for future missions.

Contrast Changes

Wave of Darkening. During the Martian spring, the contrast between dark areas and bright areas increases progressively; a maximum darkening is achieved in late spring or early Martian summer. The contrast decreases in a manner analogous to the first half of the cycle. In addition to an enhancement in contrast between bright and dark areas, there is some evidence that changes in color also occur. Changes in the polarization of sunlight scattered from the dark areas also accompany the changes in reflectivity. Secular changes in the borders of bright and dark areas probably are related; sometimes these erratic variations change large areas over a period of 2 years, but smaller secular changes over periods of months are possible. Under the best Earth-based resolution, the dark areas resolve into a leopard-skin pattern of small, dark spots, which have characteristic dimensions of a few hundred kilometers and characteristic time scales of about a week for seasonal albedo variations. The integrated albedo change in these spots is responsible for the darkening cycle.

In the biological explanation of these seasonal changes, Martian organisms inhabit the dark spots; their springtime growth, in response to increased temperatures and humidities, causes the darkening events. To test this particular hypothesis, data from the television, infrared radiometry, and infrared spectroscopy experiments will be compared and cross-correlated. Several nonbiological hypotheses have been proposed as alternatives, including one in which seasonal changes in wind patterns (caused by meridional circulation or dust devils) redistribute the particle sizes in the bright and dark areas and produce the albedo changes (Sagan and Pollack, 1969). Here, detailed correlation of dust storms with the darkening cycle is important.

In any study of the darkening cycle, it is essential that the lighting conditions be kept constant, or variations due to the scattering phase function may be misinterpreted as intrinsic albedo variations. In studying the seasonal changes, the contrast changes and changes in the reflectivity of a given area will be measured. (These two parameters are not equivalent because bright areas also may undergo albedo variations.) It is obvious that determinations of reflectivity variations require constant lighting conditions. Even for contrast measurements, there is no guarantee that the two areas in question will have the same phase function; thus, again, constant lighting conditions are desirable. A tentative statement of this requirement is the constraint that the phase angle, the illumination angle, and the reflection angle be constant within 10 deg over a 90-day period of observation. At the time of arrival of the Mariner Mars 1971 spacecraft, a variety of dark areas between +5 and −30 deg latitude will be just before, near, or after the maximum in the local darkening cycle (Focas, 1962). Primarily the second half of the darkening cycle will be viewed.

Low-resolution, Earth-based studies indicate that absolute contrast and contrast changes are greatest in the orange spectral range. Thus, an orange filter on the television camera will be used for such purposes. The amplitude of the contrast changes observed from Earth varies greatly from dark area to dark area, but some 10 to 30% is a representative figure. It is important to determine the change in contrast (with respect, say, to the large equatorial bright areas) and the change in absolute reflectivity. The intensity levels in pictures taken at different times will be compared and determined, within a few percent. Also, changes in polarization of the reflected light must be determined at least to this accuracy. To accomplish this, the way in which the vidicon characteristics change with time must be known to reasonable accuracy.

The seasonal darkening is a wave only in the statistical sense, and some areas deviate markedly from a progressive pattern (Pollack *et al.*, 1967). The 1971 arrival date will not permit close studies of such deviations, but some useful information may be obtained from the timing of the second half of the darkening cycle, which must be viewed on a global scale, rather than in a few specific regions. Global surveillance also is required to study the apparent brightening of bright areas, especially bright areas in the southern hemisphere near 50 deg latitude. These areas brighten at the same time that adjacent dark areas darken. While there are occasional frost or cloud events that also occur over these bright areas during the Martian summer, the changes in question appear to be intrinsic to the surface. The use of a blue filter may help to distinguish between these two possibilities; intrinsic changes in the surface may not show much contrast with a blue filter, but frost or clouds can be expected to show such contrast. Finally, with global coverage, data derived from the Mariner Mars 1971 variable-features investigation can be readily related to the lower-resolution, Earth-based photographs.

Secular changes, particularly variations in the boundaries between bright and dark areas, may be observable for more than the 90 days provided for the mission. Coordinate control points on a small scale will be useful in detecting such nonperiodic events. In general, the smaller dark areas that are largely surrounded by bright areas, such as Solis Lacus, exhibit the secular changes. Good spatial and temporal resolution should provide a better understanding of the relationship between the mechanisms involved in the seasonal and secular variations.

Polar Cap and Polar Cap Edge. The edge of the southern polar cap, which will have receded considerably by the time of arrival, is of great interest. Observations from earth indicate that islands of frost are left behind during the general recessions of the cap. This has been attributed to temperature or pressure differences in the terrain, or to differences in the prevailing wind velocities with terrain. Local slopes may also play a role as noted in Mariner VII pictures. The infrared radiometry experiment on Mariner Mars 1971 may help to resolve this issue. Also, the temperatures of two adjacent frost-covered areas, one of which loses its covering significantly before the other, will be compared. The albedo of the frost-free areas (i.e., whether they are bright or dark areas) and their altitudes (i.e., whether they are elevations, depressions, or some intermediate category) will be investigated. The latter parameter may be obtained from measurements from the ultraviolet spectroscopy, S-band occultation, and infrared spectroscopy experiments.

From many biological points of view, the receding polar cap is the most interesting Martian locale known. Hopefully, the edges of both the northern and the southern polar caps will be photographed.

Atmospheric Phenomena

There are two general classes of atmospheric phenomena: (1) the gaseous atmosphere, and (2) hazes or clouds in the atmosphere. These phenomena are observed and measured by the scattering and absorption that they produce on the incident solar radiation.

A great deal of interest has been centered on the vertical structure of the atmosphere and haze, which, when observed at different latitudes and as a function of season, will provide important data on the Martian atmospheric processes, perhaps including atmospheric dynamics in the polar regions. Knowledge of the vertical structure also is important in determining the physical processes involved in the formation of any haze. Data on the vertical structure can be derived by viewing the area above the limb of the planet when the atmosphere is viewed against a dark background (see Young, 1969). Pictures of the terminator can be used to assist in the determination of the structure of any thick hazes that may be observed. As one moves away from the terminator, increasingly higher altitudes are shadowed, so that the brightness distribution beyond the terminator can be a sensitive indicator of the structure of the atmosphere.

Gaseous Atmosphere. The scattering properties of the gaseous atmosphere are known, and the absolute number densities of molecules can be determined from the brightness profiles. The conversion depends on the composition of the atmosphere; however, it is expected that the measurements from the ultraviolet spectroscopy, S-band occultation, and infrared spectroscopy experiments will provide some of the needed information.

Hazes. The limb pictures acquired by Mariner VII revealed the presence of a haze in the atmosphere a few tens of kilometers above the surface. This haze exhibits spatial variations in intensity and in altitude, and, reasonably, it also may be expected to be subject to temporal variations. The optical thickness of the observed haze in the vertical direction is estimated to be only a few hundredths (Leovy, 1969) and as such would not be detectable in surface photography except at viewing angles greater than about 60 deg.

There also is some evidence for the localized presence of a thicker haze that would impair surface photography. The far-encounter pictures of Mariners VI and VII showed an extensive region of obscuration over part of the southern polar cap, and the near-encounter pictures show an area of diminished contrast at the western edge of the cap. These effects could be the result of a haze with an appreciable optical thickness. The presence of any haze with a significant optical thickness would be an important factor to the variable-features investigation of temporal variations, because variations in the haze can simulate or mask changes in both the albedo and the contrast.

Scattering from the haze can be separated from that of the gaseous atmosphere because of the unique spectral dependence exhibited by Rayleigh scattering in the gaseous atmosphere. By using successive pictures taken with filters transmitting different spectral passbands, it is possible to distinguish among those regions where Rayleigh scattering is predominant, and to determine the spectral dependence of the haze in the region in which the haze is predominant.

The scattering law for any haze is not known *a priori*, and it may not be possible to make direct quantitative measurements of the dust or aerosol densities.

Clouds. Although the recent data acquired by Mariners VI and VII failed to identify positively any clouds, numerous Earth-based observations have recorded phenomena which seem to possess cloud-like characteristics. Such observations indicate that clouds tend to form near the morning terminator and to disappear during the day. By combining measurements from the infrared radiometry, ultraviolet spectroscopy, S-band occultation, and infrared spectroscopy experiments, a reasonable understanding of the meteorology of a local point will be provided, and various alternatives for physical processes on Mars will be determined.

Two-color observations will allow a preliminary separation of clouds into the two basic types observed from Earth: (1) yellow clouds, which are presumably dust stirred up from the surface; and (2) white clouds, which are either water or carbon dioxide condensation products. Both white and yellow clouds can be expected to have lifetimes on the order of a day, and the study of their motion will provide information on circulation of the Martian atmosphere.

Observations from the infrared spectroscopy experiment may help to distinguish between water and carbon dioxide clouds. From temperature structure information, obtained from investigations of the carbon dioxide bands, occultation experiments, and determinations of the atmospheric water-vapor content, saturation conditions near the cloud can be studied. The spectra from this experiment may indicate the presence or absence of such characteristic ice features as the 12-μ absorption maxima.

Yellow dust clouds are of interest, from a strictly meteorological viewpoint, in order to study the mechanism responsible for placing surface particles into suspension in the atmosphere. The global wind patterns may be responsible; in this case, dust raising will occur over an extended area. Alternatively, dust devils may be the principal mechanism. Dust raising at a given time may take place in very localized regions, perhaps 0.1 to 1 km across, and the highest resolution would be required to observe them.

There is also a special interest in yellow clouds because they represent a possible agent for effecting surface variations. One quantitative model of the seasonal changes invokes the exchange of dust particles by global circulation or by dust devils, between dark and bright areas (Sagan and Pollack, 1969). Thus, darkening and brightening events will be correlated with removal and deposition of small dust particles, as indicated by the presence of dust clouds.

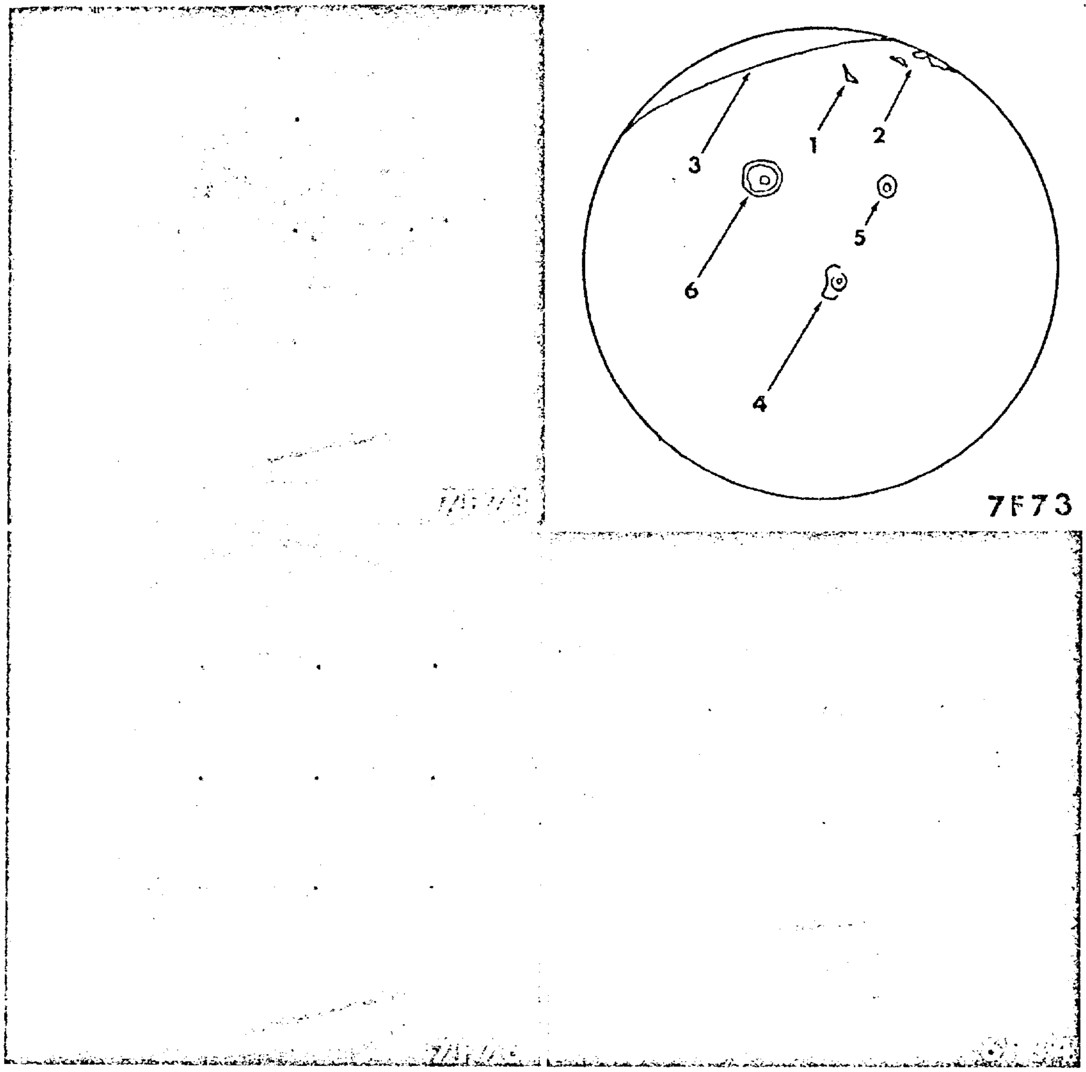

FIG. 14. Far-encounter pictures showing atmospheric and atmosphere-surface effects. Picture shutter times were: 6F34, July 30, 1969, 07:32 UT; 7F73, August 4, 1969, 11:15 UT; 7F76, August 4, 1969, 13:36 UT. Marked changes seem to have occurred, between the Mariner VI and VII flybys, in the appearance of high northern latitudes. Some of these changes are revealed by a comparison of Frames 6F34 and 7F73, which correspond to approximately the same central meridian and distance from Mars. The widespread, diffuse brightening covering much of the north polar cap region (point 3) apparently corresponds to the "polar cap hood" which has been observed from Earth at this Martian season (northern early autumn). The extent of this hood is smaller in pictures from Mariner VII than in pictures from Mariner VI. Particularly striking are several long light streaks near Nix Olympica (point 6 in Frame 7F73) and numerous circular features resembling craters, which have bright centers and dark edges. Several of the circular features exhibit one or more concentric circles similar to, but less striking than, those near Nix Olympica. Two features of this type form two of the westernmost points of the classical "W-cloud" (points 4 and 5).

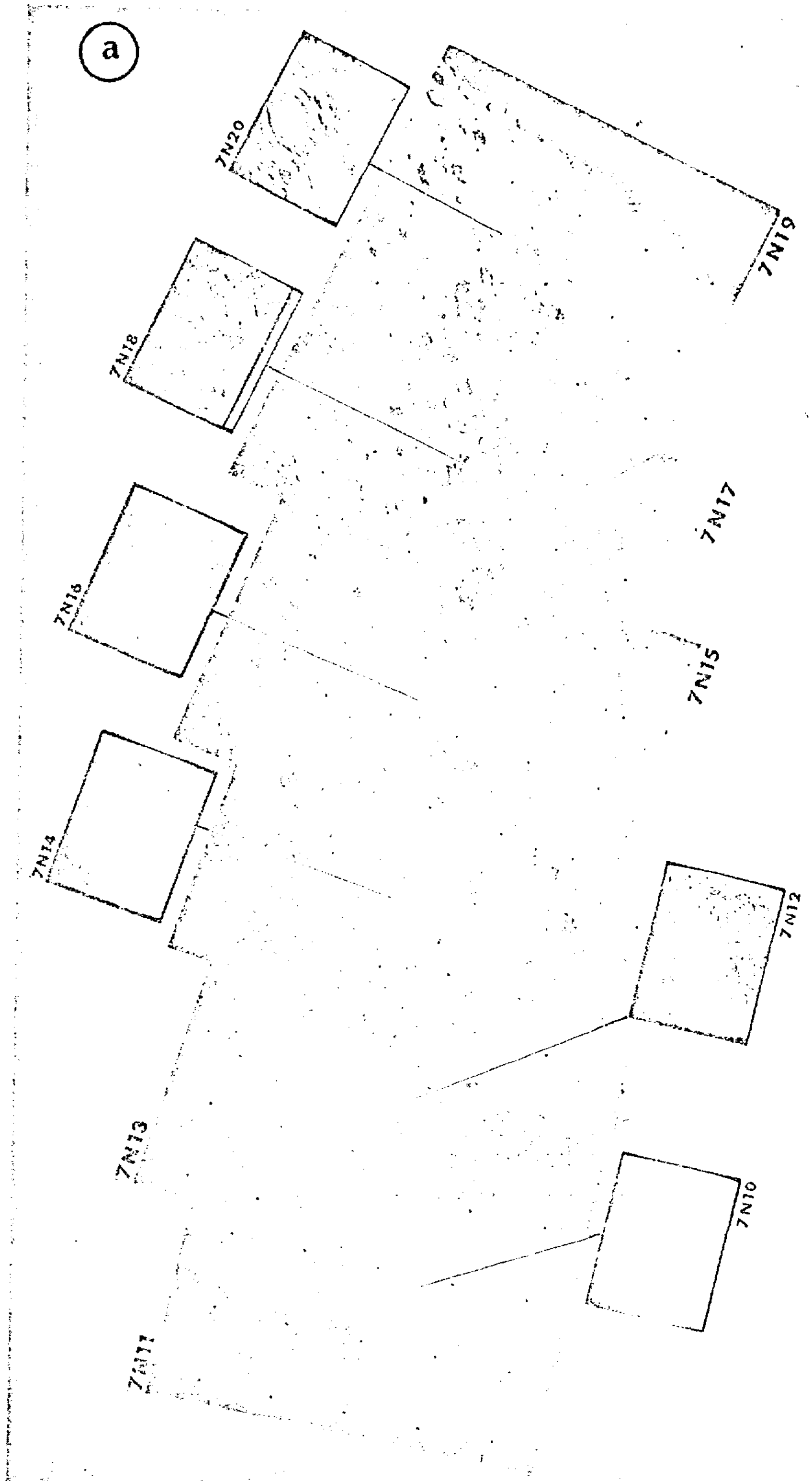

FIG. 15(a). Composite of polar cap Frames 7N10 to 7N20. Effects of automatic gain control are evident near the terminator (right) and at cap edge.

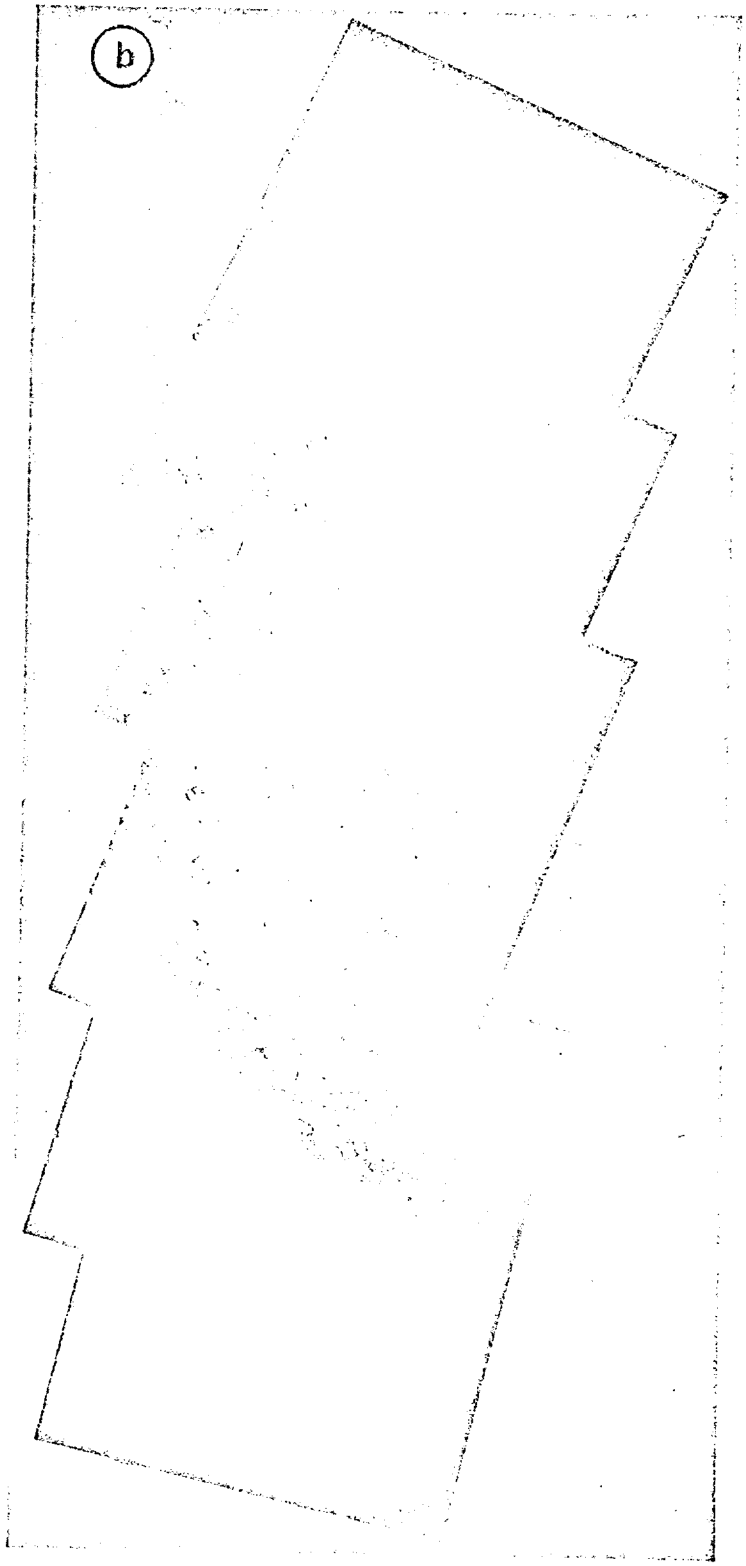

ntrol are

FIG. 15(b). Composite of polar cap Frames 7N11 to 7N19 from the wide-angle camera. The effects of automatic gain control have been partially corrected, but contrast is enhanced. The south pole lies near the parallel streaks in the lower-right corner of frame 7N17.

Some Implications of Mariners VI and VII

Because Mariners VI and VII spent a relatively short period of time (especially if we exclude from consideration the far-encounter sequence) in the vicinity of Mars, it was not expected that much new information on time-variable features would be acquired by these missions. Nevertheless, a number of new and relevant phenomena were uncovered (Leighton *et al.*, 1969). Pictures of the details of the forming polar hood (Fig. 14) suggest that detailed synoptic observations of these clouds will be of considerable interest. Similarly, observations in the W-cloud area of Tharsus-Candor (Fig. 14), combined with the history of past Earth-based observations of the region, mark it as a prime candidate for detailed time-sequence photography. The irregular and serrated nature of the edge of the retreating polar cap, as shown by Mariner VI and VII photography (Fig. 15), promises to reveal in 1971 a high-resolution history of the retreat of the cap toward the pole. Direct evidence of the existence of a high-altitude aerosol haze layer (Fig. 16) points to the advantage of observing this phenomenon over a significant time interval.

The remarkable absence of craters both large and small in Hellas (Fig. 17) suggests some erosion process of major magnitude present there and not in other parts of the Martian surface. Regardless of the nature of the Hellas erosion mechanism, detailed observations of Hellas as a function of time are clearly indicated. The unusual geometry of Nix Olympica (Fig. 14) and its Earth-based record of time variability make it a candidate for time-sequence photography. It is possible that further reduction and analyses of Mariner

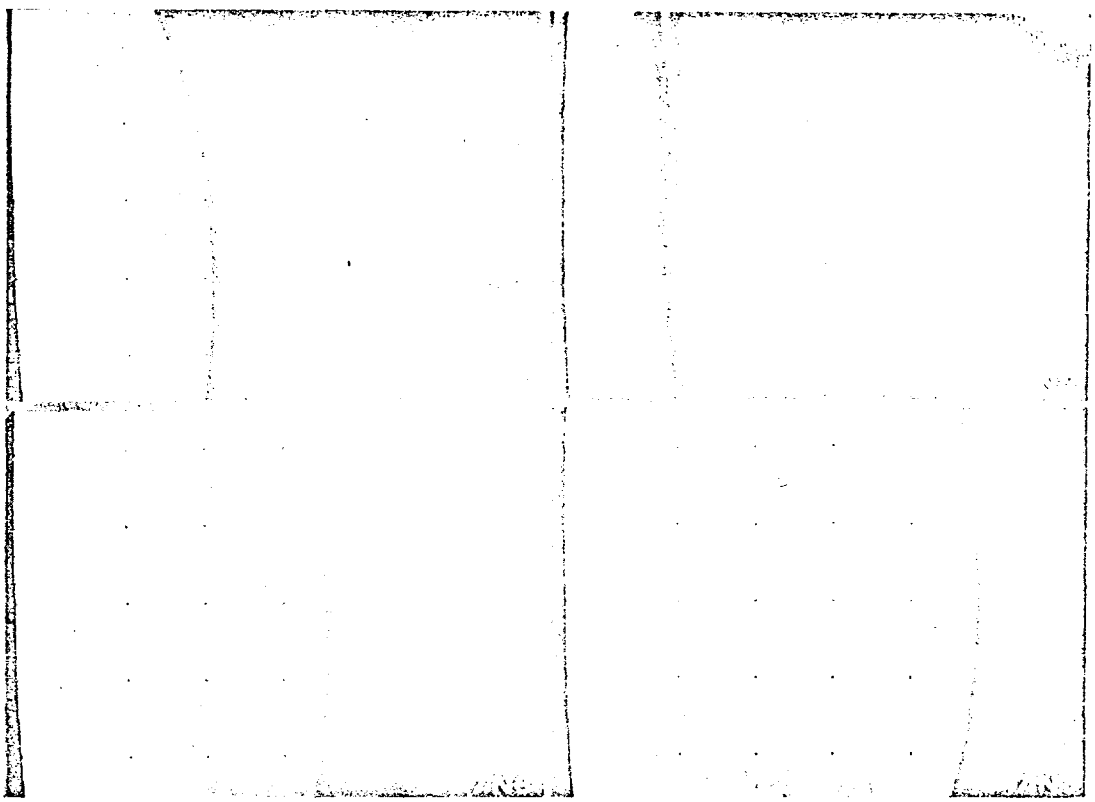

FIG. 16. Mariner VII limb Frames 7N1, 2, 3, and 5. Note the sharp haze layer adjacent to the limb in Frames 7N1, 3, and 5, and the magnified view (tenfold magnification) in Frame 7N2. The prominent, cratered dark feature in Frame 7N5 is Meridiani Sinus. North is approximately toward the right.

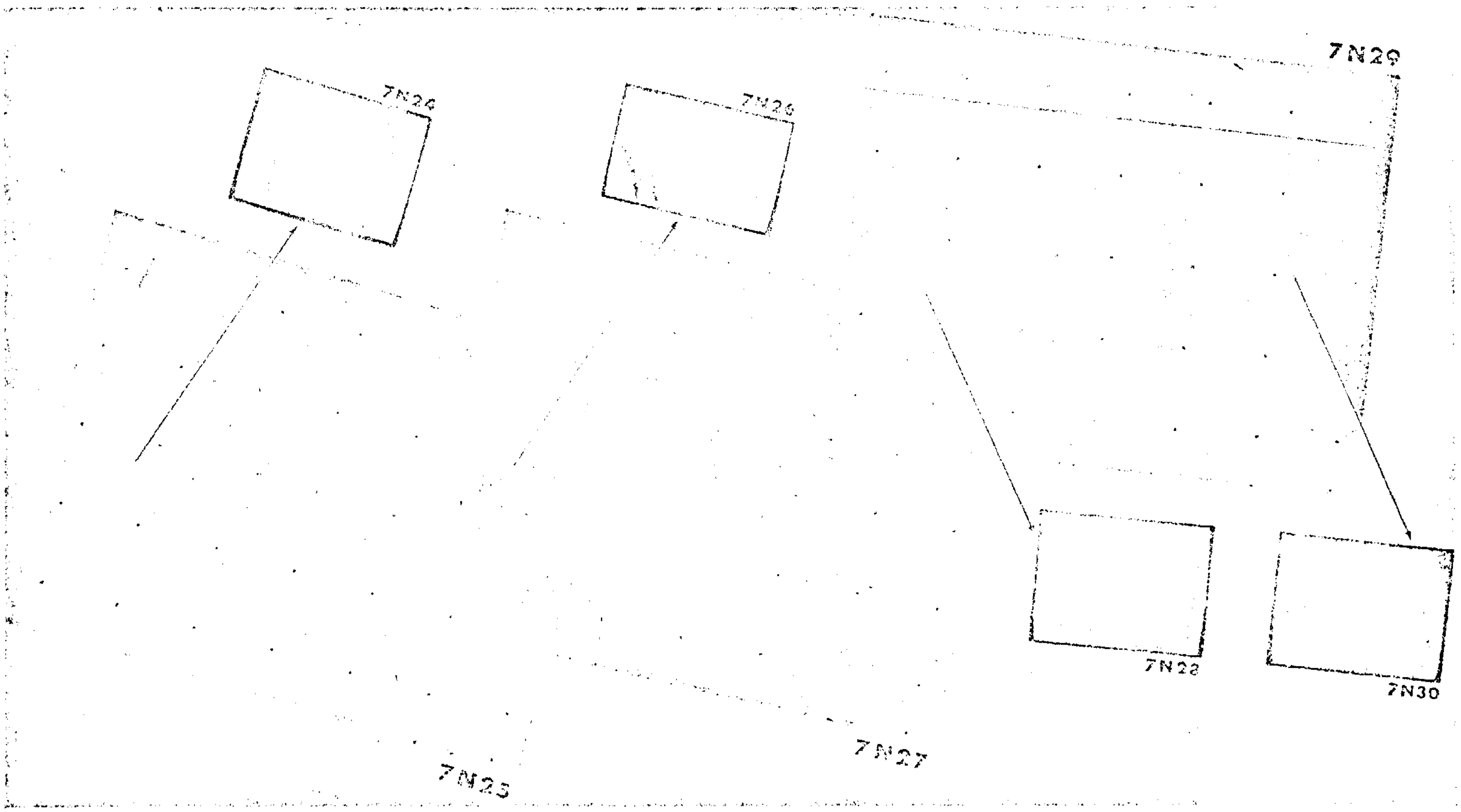

FIG. 17. Composite of seven Mariner VII pictures showing the cratered dark area, Hellespontus; the ridged, broken boundary between Hellespontus and Hellas; and the featureless terrain of the bright, circular "desert," Hellas. Large-scale variations in contrast are suppressed by automatic gain control. Lighting conditions are similar to those of Fig. 13. Frames 7N17 to 7N21. North is approximately toward the top.

VI and VII pictures will point to additional time-variable phenomena to be intensively studied during the Mariner Mars 1971 missions.

Exobiology: Search for Evidence of Life or of Biologic Habitats

What is known of the Martian environment, thus far, has suggested to some that life, if any, operates on a bare subsistence level in a marginally possible habitat, at least as measured by earthly standards. Because the low-resolution (~1 km) television camera does not reach the scale of biologically characteristic structures on Earth that might be found in the most favorable habitats, it is unlikely that orbital photography can give direct evidence of life on Mars. High-resolution photography, however, could provide evidence of anomalies such as topheaviness of tree trunks (oriented in the gravity field) or Sun following by leafy forms.

The isolated oasis is one of the possible models for a habitat (Lederberg and Sagan, 1962). The subsurface and integrated-disk temperatures of Mars are far below freezing, and most of whatever moisture has been retained by the planet must be in the form of water of hydration and deep permafrost. An oasis would be a locale of thermal activity where the crust is broken and the subsurface warmed sufficiently to release the moisture to the surface. There it is not only available to organisms, but also must dissipate into an arid atmosphere. If such oasis sites exist, they are obvious major targets for infrared hydrothermal mapping; they also could contain photographic manifestations such as clouds, volcanos, macro-relief, and related colorations.

Another possibility is that Martian life has evolved a specific adaptation to separate its water acquisition mechanism from the solar flux at the surface and to filter the photochemically destructive ultraviolet. On this model, a Martian "plant" would have leaves, encrusted with an ultraviolet filter material (iron oxide or carbonate would serve) and a tough barrier to evaporation. These plants would be joined to the bound-water or ice-harvesting mechanisms below by a deep tap root. A community of different organisms that collectively serve the same functions is also imaginable. Chemically bound water may be tappable by Martian organisms.

There is no systematic way of enumerating all possibilities; many other models are conceivable. At most, one of them is likely to survive criticism when Mariner Mars 1971 provides further indirect evidence regarding life on Mars.

Orbital Constraints

To avoid solar occultation (a present constraint on the mission), high-inclination orbits must be used. The maximum southern latitude of the subspacecraft point occurs in that part of the orbit where the spacecraft nears the longitude of the subsolar point. High Sun is desirable for measuring surface albedo, because problems associated with photometric slope effects can be avoided. Thus, basic observations of ground phenomena will be made when the spacecraft is near the subsolar point (small phase angle).

The constraint that a given area be viewed under essentially constant lighting conditions throughout the mission, when combined with the requirement for good temporal resolution (i.e., observations of the same area with successive samplings separated by no more than a few days), severely limits the number of possible orbits. To first order, only harmonic orbital periods P equal to simple fractions of the Martian rotation period, $P_♂$, are acceptable: $P=(m/n)P_♂$, where m and n are small integers. A given locale is thus viewed under similar lighting conditions once every $mP_♂=m$ Martian days. To satisfy the time requirements, $m \leq 4$.

If P were made equal to $P_♂$, only slightly more than one-half of the planet could be observed throughout the entire mission. By choosing $P \simeq (m/n)P_♂$, $m \neq n$, a rotation of subspacecraft longitudes in successive orbits is obtained. For example, if $(m/n)=\frac{3}{2}$, we see, in two successive orbits, longitudes displaced by 180 deg. However, in this case, some regions would be viewed very obliquely. An orbital period of $P \simeq (4/3) P_{\delta}$, which successively views longitudes displaced by 120 deg, overcomes this difficulty and yet is consistent with requirements for good temporal coverage of a given area ($\simeq 4$ days). Periods of less than 24 hr could entail a complete orbit without passing over Goldstone; therefore, the tape recorder could not be emptied before the next data acquisition opportunity would occur. Thus, a period $\simeq 4/3\ P_{\delta}$ appears optimal, with the caveat that the period be slightly different so as to compensate for the apparent solar motion.

Mission Profile

A nominal 32.8-hr orbit for the variable-features mission is shown in Fig. 6; viewing conditions at the beginning and at the end of the nominal 90-day lifetime are indicated. A typical sequence begins a few hours after apoapsis, early in the mission. After the morning terminator of Mars enters the scan platform's field of view, five or six full-disk pictures of the planet are taken by the wide-angle camera at intervals of about 1 hr. Experiments of opportunity with the narrow-angle camera also may be performed. If possible, these near-apoapsis pictures will be played back before the near-periapsis photography; this can be accomplished in less than 1 hr per frame using a 2-kbps rate and the 85-ft antennas of the Deep Space Network. At the beginning of the mission, the spacecraft passes local Martian noon (high Sun elevation angle) approximately 1 hr before periapsis passage at an altitude of 5000 to 7000 km. Because the orbit is a $\frac{4}{3}$ harmonic of the Martian rotation period, the spacecraft will pass over this same region at high Sun every three orbits. By slewing the scan platform and taking wide-angle pictures every 84 sec, it is possible to build up overlapping coverage of a large part of each 120-deg region. Experiments of opportunity with the narrow-angle camera would also be performed at this time. The pictures must be stored and subsequently played back. If the spacecraft is over the 210-ft antenna (which occurs approximately each third orbit), at least some of the data could be played back at 16.2 kbps during the 20 to 30 min before periapsis photography. Ordinarily, playback will occur after periapsis passage.

Three or four pictures of the evening terminator and limb will be obtained beginning about 30 min before periapsis passage. About 18 min before periapsis passage, terminator pictures of selected areas previously recorded near high Sun will be obtained by the wide- or narrow-angle cameras. At periapsis passage, three or four vertical wide-angle pictures of the terminator will be taken. It is desirable to play back all stored pictures before the next near-apoapsis photographic sequence begins. Photography of Phobos and Deimos also will take place at appropriate times during the mission. Because of the apparent solar motion, the above sample photographic sequence will vary into the mission (see Fig. 6), e.g., the time of taking high-Sun pictures. Typical photographic sequencing "footprints" for this mission are displayed in Fig. 18.

Because high priority is placed on global coverage to observe the seasonal changes, a small sacrifice in resolution is made to achieve this goal. For example, with orbital periapsis at the evening terminator and a posigrade orbit, observations could be made when the spacecraft is nearest the subsolar point with a linear resolution degradation of only about a factor of 3 (see Fig. 6). Under these circumstances, the Martian semidiameter, as seen from the spacecraft, is about 22 deg, and with the wide-angle camera's field of view (11 by 14 deg), about 10 overlapping pictures will provide complete coverage of the illuminated disk. Because the maximum number of pictures that can be stored on tape is about 32, a complete set of pictures from much lower altitudes cannot be obtained. The remaining pictures could be used for other purposes, e.g., complete coverage with a second filter, or concomitant narrow-angle pictures interspersed among the wide-angle pictures. To obtain a set of overlapping pictures, the platform must be properly slewed between frames.

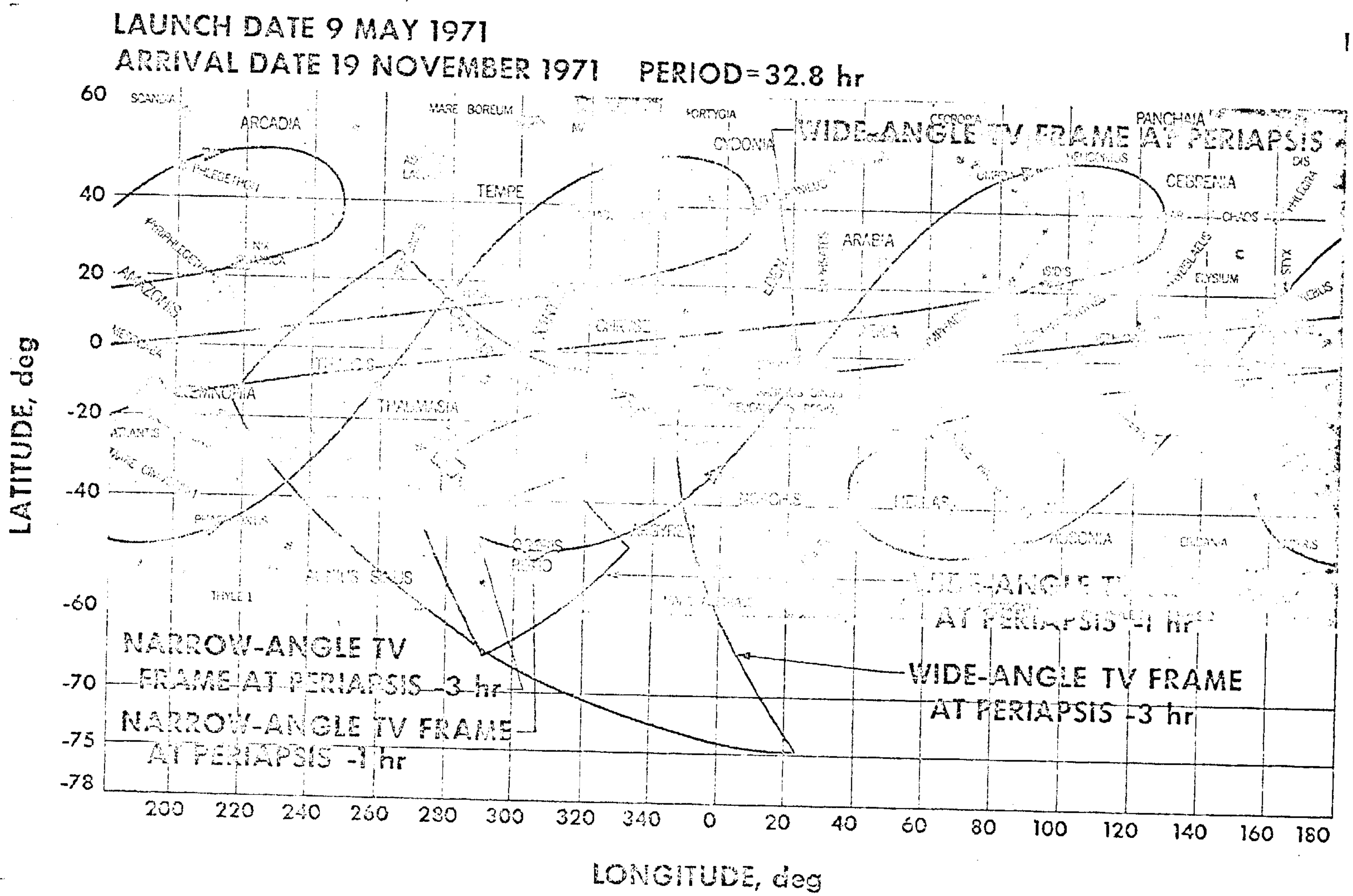

FIG. 18. Mars map showing 32.8-hr orbit ground tracks and wide- and narrow-angle camera coverage.

3. *Martian Satellites: Phobos and Deimos*

An important byproduct of both the fixed- and variable-feature missions is the opportunity to photograph, in fair detail, the satellites of Mars. There are three general views as to their nature—all speculative: they may be debris left over from the formation of Mars, objects captured from the asteroid belt or elsewhere in the solar system (they are about the size of the Apollo objects), or, least likely, artificial satellites of an extinct Martian civilization, as proposed by Shklovskii. Whichever one of these possibilities is correct, the satellites are of major scientific interest.

Apart from their orbital properties, virtually nothing is known about Phobos and Deimos—the radii are estimated by assuming, rather arbitrarily, an albedo and by deducing radii from their apparent magnitudes. The satellites are so small that they are well below the limiting size at which hydrostatic equilibrium forms spherical figures for natural objects in the solar system. As a result, they should have asymmetrical shapes, as is known to be the case even for some asteroids considerably larger in size.

Rough calculations show that the proposed 12- and 32.8-hr orbits will approach within 6000 to 7000 km of the orbit of Phobos; the 12-hr orbit will approach equally near the orbit of Deimos (although viewing may involve rotation off Sun/Canopus lock). Such close approaches will occur once each orbit. This gives a line-pair spacing of about 150 m for the narrow-angle camera, or about 75 to 150 lines across the satellites. It would then be possible to compile a photographic atlas of Phobos and of Deimos with more resolution elements in each than the best contemporary Earth-based photographic maps of Mars.

For a 12-msec shutter speed, there is no motion smearing due to rotation, even if Phobos and Deimos have rotation periods as short as that of the fastest rotating asteroid, Icarus. In most cases, about 30 narrow-angle pictures near closest approach are adequate for a complete map. For a rotation period of 2 hr, this corresponds to a picture every few minutes for only 1 hr. The shapes of the range curves, computed by John Freeman of the Jet Propulsion Laboratory, show the minima to be relatively flat over time intervals of 1 or 2 hr.

Continuing observations of these satellites could be useful in calibrating the television subsystem (which is particularly important in order to accomplish the variable-features investigation), if extensive observations of Phobos and Deimos are performed over the entire rotation cycle of these satellites and over 180 deg in phase angles. Very close approaches are not required for calibration.

In addition to photographic reconnaissance of Phobos and Deimos, the nontelevision experiments on Mariner Mars 1971 will be directed at these satellites. As a result, it may be possible to obtain the following information about Phobos and Deimos: their topography, geometrical figures, periods of rotation, obliquities, albedos as a function of wavelength and position, polarizations at large phase angles as a function of position, surface temperature distributions, thermal inertias, surface powder packing fractions, and ultraviolet and infrared spectra. Eclipses of the Sun by Mars, as seen from Phobos and Deimos, should be fairly common during the mission, and infrared radiometric observations of the satellites during such eclipses should give additional information on thermal inertias, as well as on surface thermal anomalies. If the range is sufficiently small, perturbations of the orbiters by Phobos and Deimos may give a reliable estimate of the masses of the Martian satellites and therefore of their densities—a possible clue to their origins.

In a variety of fundamental respects, observations of Phobos and Deimos provide important controls for observations of Mars. For example, a serious question in the study of cratering statistics of Mars is the extent to which erosion processes have obliterated craters formed during earlier cratering epochs. One erosion mechanism that has been discussed is wind-blown dust. Since Phobos and Deimos very likely have no atmospheres at all, they can have no wind-blown dust. If their ages are comparable to those of Mars, they provide a control impact counter in the absence of wind-blown dust. Another possibility worth investigating is whether the scattered light from Mars is low enough to permit probing the Martian atmosphere by observing occultation by Mars of Phobos and Deimos.

It is conceivable that the Mariner Mars 1971 missions can convert Phobos and Deimos from objects about which we know virtually nothing into objects about which we know a great deal.

V. Relationship with Other Experiments

Results from the television experiment will be compared with the results from the other experiments aboard Mariner Mars 1971, with a productive exchange of data. Some of the most interesting interfaces are discussed in the following paragraphs.

Some hypotheses of the seasonal darkening invoke a relationship with high temperatures and humidities. Two-dimensional maps obtained from the infrared radiometry and infrared spectroscopy experiments, at the same time and of the same area as the set of overlapping television frames, will permit a close examination of biological models of the wave of darkening.

Measurements of white clouds obtained from the infrared spectroscopy experiment may help to distinguish carbon dioxide clouds from water clouds. Observations of clouds by the infrared spectroscopy, S-band occultation, and ultraviolet spectroscopy experiments may permit determinations of their altitudes.

Altitude mapping from the infrared spectroscopy, ultraviolet spectroscopy, and the S-band occultation experiments will indicate how albedo is correlated with elevation, over a wide range of latitudes.

Temperature maps of the polar cap areas will help to indicate whether areas that become frost-free are cooler or warmer than adjacent regions that retain their frost deposits longer. Determinations of the altitude of the frost-free regions by the ultraviolet spectroscopy, S-band occultation, and infrared spectroscopy experiments also will be made.

Studies of the collar near the polar cap edge by the infrared radiometry and infrared spectroscopy experiments will provide data regarding its reality and composition.

To check wind-blown dust models of seasonal changes, the meridional temperature gradient as determined by the infrared radiometer will be correlated with seasonal changes.

Acknowledgments

Although all team members contributed to and reviewed the text of this article, the principal contributors were J. McCauley, fixed features (geology); W. Hartmann (craters); G. de Vaucouleurs and M. Davies (geodesy/cartography); C. Sagan, J. Pollack, and W. Thompson, variable features; C. Sagan, Phobos and Deimos; and D. Norris, hardware. Thanks are due to Mrs. Ermine van der Wyk of the Jet Propulsion Laboratory for assembly and review of the multiauthored material.

References

Borgeson, W. T. (1966). "The Use of Lunar Orbiter Data in Plotters Available to the U.S. Geological Survey," pp. 33–48. Lunar Orbiter—Image Analysis Studies Rept., U.S. Geol. Survey Open File Report.

Carey, W. S. (1962). Scale of geotectonic phenomena. *J. Geol. Soc. India* **3**, 97–105.

Chapman, C. R., Pollack, J. B., and Sagan, C. (1969). An analysis of the Mariner 4 cratering statistics. *Astron. J.* **74**, 1039.

Focas, J. H. (1962). Seasonal evolution of the fine structure of the dark areas of Mars. *Planet. Space Sci.* **9**, 371.

Keene, G. C. (1965). "Lunar Orbiter Photo Study Z-3841." p. 137. Eastman Kodak Company, Rochester, New York.

Lederberg, J., and Sagan, C. (1962). Microenvironments for life on Mars. *Proc. Natl. Acad. Sci.* **48**, 1473–1475.

Leighton, R. B., *et al.* (1969). Mariner 6 and 7 television pictures: Preliminary analysis. *Science* **166**, 49–67.

Leovy, C. (1969). Mariner Mars 1969 Press Conference, held in Washington, D.C., September 11, 1969.

McCauley, J. F. (1967). The nature of the lunar surface as determined by systematic geologic mapping. *In* Mantles of the Earth and Terrestrial Planets," 431–460. Interscience, London, New York, Sydney.

Pollack, J. B., Greenberg, E., and Sagan, C. (1967). A statistical analysis of the Martian wave of darkening and related phenomena. *Planet. Space Sci.* **15**, 817.

Rowan, L. C., McCauley, J. F., and Holm, E. A. (In press). "Lunar Terrain Mapping and Relative Roughness Analysis." U.S. Geol. Survey Prof. Paper 599-G.

Sagan, C., and Pollack, J. B. (1969). Windblown dust on Mars. *Nature* **223**, 791–794.

Sharp, R. P., Murray, B. C., Leighton, R. B. (1967). "Mariner IV Pictures of Mars." Jet Propulsion Lab. Tech. Rept. 32–884, Part I, Appendix J, pp. 163–167.

Shoemaker, E. M., and Hackman, R. J. (1962). Stratigraphic basis for a lunar time scale. *In* "The Moon," pp. 289–300. Academic Press, London & New York.

de Vaucouleurs, G. (1963). Precision mapping of Mars. 1962 Liege Symposium on "La Physique des Planetes," *Mem. Soc. Roy. Sci. Liege* **7**, 369; see also *Sky and Telescope* **30**, 196.

de Vaucouleurs, G. (1964). Geometric and photometric parameters of the terrestrial planets. *Icarus* **3**, 187.

de Vaucouleurs, G. (1970). "Cartography of the Planet Mars." Gordon and Breach, New York & London.

Wilhelms, D. E. in press. "Summary of Lunar Stratigraphy Telescopic Observations." U.S. Geol. Survey Prof. Paper 599-F.

Wilhelms, D. E., and McCauley, J. F. (1969). "Geologic Map of the Near Side of the Moon." U.S. Geological Survey Open File Report (in press as I series map, scale 1:5,000,000).

Wu, S. S. C. (1969). Photogrammetry of Apollo 8 photographs. *In* "Initial Photographic Analysis, Analysis of Apollo 8 Photographs and Visual Observations." NASA SP-201, National Aeronautics and Space Administration, Washington, D.C.

Young, A. T. (1969). High-resolution photometry of a thin planetary atmosphere. *Icarus* **11**, 1–23.